leads to ROS accumulation. In addition, MnSOD, which plays a key role in protecting cells from oxidative damage, was up-regulated in core-expressing cells, reflecting ROS increase in the cells. Several protein chaperons such as HSP70 and GrpE-like protein co-chaperon were also identified as up-regulated proteins. Because these proteins are known to be important in the mitochondrial protein-import mechanisms, the modulated expression of these proteins may be associated with the different expressions of the identified mitochondrial proteins.

Prohibitin, a mitochondrial protein chaperon, was identified as an up-regulated protein in core-expressing cells. Prohibitin is a ubiquitously expressed and highly conserved protein that was originally determined to play a predominant role in inhibiting cell-cycle progression and cellular proliferation by attenuating DNA synthesis.[20,25] Prohibitin is present in the nucleus and interacts with transcription factors that are important in cell cycle progression. In core-expressing cells used in this study, prohibitin was also detected in the nucleus and its expression level was also higher than that in control Hepswx cells or HepG2 cells (data not shown). The growth rate of core-expressing cells, however, was similar to that of control cells (data not shown). The physiological significance of the high expression level of prohibitin in the nucleus remains to be determined, but it may be related to enhanced apoptosis by Fas ligand, as shown by Ruggieri et al.,[16] because prohibitin interacts with E2F, Rb, and p53 and modulates the transcription activity of these factors and induces apoptosis.[26,27]

Mitochondrial prohibitin acts as a protein chaperon by stabilizing newly synthesized mitochondrial translation products through direct interaction.[21] We examined the interaction between prohibitin and mitochondrially encoded subunit II of COX and found a suppressed interaction between these proteins in core-expressing cells. In addition, there are several studies that showed the association of prohibitin with the assembly of mitochondrial respiratory complex I as well as complex IV (COX).[21,28] Complex I also consists of both nuclear- and mitochondrial-DNA-encoded subunits; therefore, it is probable that the assembly and function of complex I are impaired by the core protein. We attempted to examine the interaction of prohibitin with the mitochondrial DNA-encoded subunit of complex I, but commercially available antibodies against this subunit could not detect the protein itself by immunoblotting (data not shown). With respect to the complex I function, we found a decreased complex I activity in core-expressing cells (H. Miyoshi et al., manuscript in preparation). Other groups have also shown that complex I activity is decreased in the liver of transgenic mice harboring HCV core and envelope genes[9] as well as in cultured cells.[29] From these findings, the interaction between prohibitin and the core protein may impair the function of complex I as well as complex IV, leading to an increase in ROS production. In fact, the suppression of the prohibitin function is shown to result in an increased production of ROS,[30] a phenomenon observed in core-expressing cells used in this study (Miyoshi et al., in prep.) as well as in the liver of core-gene transgenic mice.[7,8] Interestingly, Berger and Yaffe[31] showed that loss of function of prohibitin leads to an altered mitochondrial morphology, that is, the loss of the normal reticular morphology and organized mitochondrial distribution. In hepatocytes from the core-gene transgenic mice, we observed a change in morphology of mitochondria, a disappearance of the double structure of mitochondrial membranes.[2] These changes in mitochondrial morphology are somewhat different, but the dysfunction of prohibitin may be responsible for the morphological abnormality of mitochondria observed in the core-gene transgenic mice.

We concluded that prohibitin overexpression is due to increased stability induced by the interaction with the core protein. In this study we showed that prohibitin might be degraded by proteasome, although we could not detect ubiquitinated forms of prohibitin. If the degradation is mediated by ubiquitin as reported,[23] it is possible that the interaction with the core protein interferes with ubiquitin-binding and protects prohibitin from degradation by proteasome. Some posttranslational protein modifications such as phosphorylation are other possible factors for the stabilization, because prohibitin can be serine-phosphorylated[32]; however, in our examination no serine/threonine/tyrosine phosphorylation of prohibitin was detected in core-expressing cells (data not shown). Thus far, there are no studies showing that prohibitin stabilization leads to a suppressed function as a mitochondrial chaperon. Therefore, this finding is novel and noteworthy because the prohibitin expression level has been considered to be proportional to the chaperon function. Prohibitin is highly expressed in several human tumors.[33,34] In addition, a 2D-PAGE of the hepatoma cell line HCC-M identified prohibitin as a positively regulated protein.[35] In these studies, the mechanism of prohibitin overexpression was not elucidated, but considering that prohibitin is associated with the inhibition of cell proliferation, the function of prohibitin is suppressed by stabilization by some molecules in the tumor, similar to the mechanism we suggest in the current study.

In addition to HepG2 cells constitutively expressing the core protein, increased prohibitin expression levels were also found in livers of core-gene transgenic mice.

The difference in expression levels between the transgenic mice and nontransgenic littermates, however, was a little bit smaller than that in the studies of HepG2 cells. This may be due to the low expression level of the core protein in the transgenic mice compared with that in core-expressing HepG2 cells because the expression level of prohibitin was proportionally increased to that of the core protein as shown in this study (Fig. 2D). Otherwise, there might be some *in vivo* mechanism for suppressing prohibitin expression in mice.

In this study, COX subunit IV as well as II were found to interact with prohibitin (Fig. 5A). Although there are no studies demonstrating that prohibitin also works as chaperon for nuclear DNA-encoded mitochondrial proteins as far as we investigated, knockdown of prohibitin expression by siRNA led to decreases in expression levels of both nuclear (COX IV, VIb) and mitochondrial (COX I, II) DNA-encoded subunits in mitochondria (Fig. 5B and Supporting Figs. 1 and 2). We showed that COX IV interacts with prohibitin (Fig. 4), suggesting that prohibitin also works for stable expression of nuclear DNA-encoded COX IV. Degrees of decrease in COX IV and VIb expression, however, were smaller than those in I and II. Prohibitin might contribute to stabilization of COX IV and VIb by mechanism(s) other than chaperon function. Steglich et al.[36] showed that prohibitin regulates protein degradation by the m-AAA protease in mitochondria. Recently, Da Cruz et al.[37] showed that SLP-2, a member of the stomatin gene family, interacts with prohibitin and regulates the expression of mitochondrial proteins such as COX IV and ND6 of complex I encoded by nuclear DNA by AAA proteases. In view of these findings, COX IV and VIb expression in mitochondria is dependent on prohibitin but other factors may also be involved in the attainment of stable expression of these subunits. The expression levels of COX II and IV in the whole-cell lysates were not so drastic among cell samples (Fig. 5A) compared to those in the mitochondria (Fig. 5B). The reason is not clear, but it is possible that redundant proteins such as improperly folded proteins by lack of chaperons were included in the whole-cell lysates.

In summary, we analyzed mitochondrial proteins in core-expressing HepG2 cells by proteomics analysis and identified prohibitin as an up-regulated protein. The dysfunction of prohibitin induced by the core protein may lead to ROS overproduction in the mitochondrion, which plays a key role in the pathogenesis of chronic hepatitis C. The restoration of prohibitin function might be a therapeutic option for correcting the dysregulated assembly and dysfunction of mitochondrial respiratory chain complexes.

Acknowledgment: We thank S. Shinzawa, M. Yahata, and S. Yoshizaki for technical assistance.

References

1. Suzuki R, Suzuki T, Ishii K, Matsuura Y, Miyamura T. Processing and functions of Hepatitis C virus proteins. Intervirology 1999;42:145-152.
2. Moriya K, Fujie H, Shintani Y, Yotsuyanagi H, Tsutsumi T, Ishibashi K, et al. The core protein of hepatitis C virus induces hepatocellular carcinoma in transgenic mice. Nat Med 1998;4:1065-1067.
3. Naas T, Ghorbani M, Alvarez-Maya I, Lapner M, Kothary R, De Repentigny Y, et al. Characterization of liver histopathology in a transgenic mouse model expressing genotype 1a hepatitis C virus core and envelope proteins 1 and 2. J Gen Virol 2005;86:2185-2196.
4. Machida K, Cheng KT, Lai CK, Jeng KS, Sung VM, Lai MM. Hepatitis C virus triggers mitochondrial permeability transition with production of reactive oxygen species, leading to DNA damage and STAT3 activation. J Virol 2006;80:7199-7207.
5. Suzuki R, Sakamoto S, Tsutsumi T, Rikimaru A, Tanaka K, Shimoike T, et al. Molecular determinants for subcellular localization of hepatitis C virus core protein. J Virol 2005;79:1271-1281.
6. Schwer B, Ren S, Pietschmann T, Kartenbeck J, Kaehlcke K, Bartenschlager R, et al. Targeting of hepatitis C virus core protein to mitochondria through a novel C-terminal localization motif. J Virol 2004;78:7958-7968.
7. Moriya K, Nakagawa K, Santa T, Shintani Y, Fujie H, Miyoshi H, et al. Oxidative stress in the absence of inflammation in a mouse model for hepatitis C virus-associated hepatocarcinogenesis. Cancer Res 2001;61:4365-4370.
8. Okuda M, Li K, Beard MR, Showalter LA, Scholle F, Lemon SM, et al. Mitochondrial injury, oxidative stress, and antioxidant gene expression are induced by hepatitis C virus core protein. Gastroenterology 2002;122:366-375.
9. Korenaga M, Wang T, Li Y, Showalter LA, Chan T, Sun J, et al. Hepatitis C virus core protein inhibits mitochondrial electron transport and increases reactive oxygen species (ROS) production. J Biol Chem 2005;280:37481-37488.
10. Diamond DL, Jacobs JM, Paeper B, Proll SC, Gritsenko MA, Carithers RL Jr, et al. Proteomic profiling of human liver biopsies: hepatitis C virus-induced fibrosis and mitochondrial dysfunction. HEPATOLOGY 2007;46:649-657.
11. Moriya K, Yotsuyanagi H, Shintani Y, Fujie H, Ishibashi K, Matsuura Y, et al. Hepatitis C virus core protein induces hepatic steatosis in transgenic mice. J Gen Virol 1997;78(Pt 7):1527-1531.
12. Moriya K, Todoroki T, Tsutsumi T, Fujie H, Shintani Y, Miyoshi H, et al. Increase in the concentration of carbon 18 monounsaturated fatty acids in the liver with hepatitis C: analysis in transgenic mice and humans. Biochem Biophys Res Commun 2001;281:1207-1212.
13. Fujie H, Yotsuyanagi H, Moriya K, Shintani Y, Tsutsumi T, Takayama T, et al. Steatosis and intrahepatic hepatitis C virus in chronic hepatitis. J Med Virol 1999;59:141-145.
14. Cho WC. Contribution of oncoproteomics to cancer biomarker discovery. Mol Cancer 2007;6:25.
15. Lescuyer P, Strub JM, Luche S, Diemer H, Martinez P, Van Dorsselaer A, et al. Progress in the definition of a reference human mitochondrial proteome. Proteomics 2003;3:157-167.
16. Ruggieri A, Harada T, Matsuura Y, Miyamura T. Sensitization to Fas-mediated apoptosis by hepatitis C virus core protein. Virology 1997;229:68-76.
17. Okado-Matsumoto A, Fridovich I. Subcellular distribution of superoxide dismutases (SOD) in rat liver: Cu,Zn-SOD in mitochondria. J Biol Chem 2001;276:38388-38393.
18. Murakami K, Ishii K, Ishihara Y, Yoshizaki S, Tanaka K, Gotoh Y, et al. Production of infectious hepatitis C virus particles in three-dimensional cultures of the cell line carrying the genome-length dicistronic viral RNA of genotype 1b. Virology 2006;351:381-392.

19. Shevchenko A, Wilm M, Vorm O, Mann M. Mass spectrometric sequencing of proteins silver-stained polyacrylamide gels. Anal Chem 1996;68: 850-858.
20. Mishra S, Murphy LC, Murphy LJ. The prohibitins: emerging roles in diverse functions. J Cell Mol Med 2006;10:353-363.
21. Nijtmans LG, de Jong L, Artal Sanz M, Coates PJ, Berden JA, Back JW, et al. Prohibitins act as a membrane-bound chaperone for the stabilization of mitochondrial proteins. EMBO J 2000;19:2444-2451.
22. Back JW, Sanz MA, De Jong L, De Koning LJ, Nijtmans LG, De Koster CG, et al. A structure for the yeast prohibitin complex: structure prediction and evidence from chemical crosslinking and mass spectrometry. Protein Sci 2002;11:2471-2478.
23. Thompson WE, Ramalho-Santos J, Sutovsky P. Ubiquitination of prohibitin in mammalian sperm mitochondria: possible roles in the regulation of mitochondrial inheritance and sperm quality control. Biol Reprod 2003; 69:254-260.
24. Fontanesi F, Soto IC, Horn D, Barrientos A. Assembly of mitochondrial cytochrome c-oxidase, a complicated and highly regulated cellular process. Am J Physiol Cell Physiol 2006;291:C1129-C1147.
25. Mishra S, Murphy LC, Nyomba BL, Murphy LJ. Prohibitin: a potential target for new therapeutics. Trends Mol Med 2005;11:192-197.
26. Fusaro G, Dasgupta P, Rastogi S, Joshi B, Chellappan S. Prohibitin induces the transcriptional activity of p53 and is exported from the nucleus upon apoptotic signaling. J Biol Chem 2003;278:47853-47861.
27. Joshi B, Ko D, Ordonez-Ercan D, Chellappan SP. A putative coiled-coil domain of prohibitin is sufficient to repress E2F1-mediated transcription and induce apoptosis. Biochem Biophys Res Commun 2003;312:459-466.
28. Bourges I, Ramus C, Mousson de Camaret B, Beugnot R, Remacle C, Cardol P, et al. Structural organization of mitochondrial human complex I: role of the ND4 and ND5 mitochondria-encoded subunits and interaction with prohibitin. Biochem J 2004;383:491-499.
29. Piccoli C, Scrima R, Quarato G, D'Aprile A, Ripoli M, Lecce L, et al. Hepatitis C virus protein expression causes calcium-mediated mitochondrial bioenergetic dysfunction and nitro-oxidative stress. HEPATOLOGY 2007;46:58-65.
30. Theiss AL, Idell RD, Srinivasan S, Klapproth JM, Jones DP, Merlin D, et al. Prohibitin protects against oxidative stress in intestinal epithelial cells. FASEB J 2007;21:197-206.
31. Berger KH, Yaffe MP. Prohibitin family members interact genetically with mitochondrial inheritance components in Saccharomyces cerevisiae. Mol Cell Biol 1998;18:4043-4052.
32. Ross JA, Nagy ZS, Kirken RA. The PHB1/2 phosphocomplex is required for mitochondrial homeostasis and survival of human T cells. J Biol Chem 2008;283:4699-4713.
33. Coates PJ, Nenutil R, McGregor A, Picksley SM, Crouch DH, Hall PA, et al. Mammalian prohibitin proteins respond to mitochondrial stress and decrease during cellular senescence. Exp Cell Res 2001;265:262-273.
34. Asamoto M, Cohen SM. Prohibitin gene is overexpressed but not mutated in rat bladder carcinomas and cell lines. Cancer Lett 1994;83:201-207.
35. Seow TK, Ong SE, Liang RC, Ren EC, Chan L, Ou K, et al. Two-dimensional electrophoresis map of the human hepatocellular carcinoma cell line, HCC-M, and identification of the separated proteins by mass spectrometry. Electrophoresis 2000;21:1787-1813.
36. Steglich G, Neupert W, Langer T. Prohibitins regulate membrane protein degradation by the m-AAA protease in mitochondria. Mol Cell Biol 1999; 19:3435-3442.
37. Da Cruz S, Parone PA, Gonzalo P, Bienvenut WV, Tondera D, Jourdain A, et al. SLP-2 interacts with prohibitins in the mitochondrial inner membrane and contributes to their stability. Biochim Biophys Acta 2008;1783: 904-911.

JOURNAL OF VIROLOGY, Oct. 2009, p. 10427–10436 Vol. 83, No. 20
0022-538X/09/$08.00+0 doi:10.1128/JVI.01035-09

Cochaperone Activity of Human Butyrate-Induced Transcript 1 Facilitates Hepatitis C Virus Replication through an Hsp90-Dependent Pathway▽

Shuhei Taguwa,[1] Hiroto Kambara,[1] Hiroko Omori,[2] Hideki Tani,[1] Takayuki Abe,[1] Yoshio Mori,[1] Tetsuro Suzuki,[3] Tamotsu Yoshimori,[2] Kohji Moriishi,[1] and Yoshiharu Matsuura[1]*

Department of Molecular Virology[1] and Department of Cellular Regulation,[2] Research Institute for Microbial Diseases, Osaka University, Osaka, and Department of Virology II, National Institute of Infectious Diseases, Tokyo,[3] Japan

Received 21 May 2009/Accepted 27 July 2009

Hepatitis C virus (HCV) nonstructural protein 5A (NS5A) is a component of the replication complex consisting of several host and viral proteins. We have previously reported that human butyrate-induced transcript 1 (hB-ind1) recruits heat shock protein 90 (Hsp90) and FK506-binding protein 8 (FKBP8) to the replication complex through interaction with NS5A. To gain more insights into the biological functions of hB-ind1 in HCV replication, we assessed the potential cochaperone-like activity of hB-ind1, because it has significant homology with cochaperone p23, which regulates Hsp90 chaperone activity. The chimeric p23 in which the cochaperone domain was replaced with the p23-like domain of hB-ind1 exhibited cochaperone activity comparable to that of the authentic p23, inhibiting the glucocorticoid receptor signaling in an Hsp90-dependent manner. Conversely, the chimeric hB-ind1 in which the p23-like domain was replaced with the cochaperone domain of p23 resulted in the same level of recovery of HCV propagation as seen in the authentic hB-ind1 in cells with knockdown of the endogenous hB-ind1. Immunofluorescence analyses revealed that hB-ind1 was colocalized with NS5A, FKBP8, and double-stranded RNA in the HCV replicon cells. HCV replicon cells exhibited a more potent unfolded-protein response (UPR) than the parental and the cured cells upon treatment with an inhibitor for Hsp90. These results suggest that an Hsp90-dependent chaperone pathway incorporating hB-ind1 is involved in protein folding in the membranous web for the circumvention of the UPR and that it facilitates HCV replication.

Hepatitis C virus (HCV) is the major causative agent of non-A, non-B hepatitis in humans and infects approximately 170 million people worldwide (64). HCV belongs to the genus *Hepacivirus* of the family *Flaviviridae* and is classified into six major genotypes (39). The virus forms small, round, enveloped particles and possesses a genome consisting of a single positive-stranded RNA with a nucleotide length of 9.6 kb. The viral genome encodes a single precursor polyprotein consisting of approximately 3,000 amino acids, which in turn is posttranslationally processed into 10 viral proteins by host and viral proteases. The structural proteins are cleaved from the N-terminal one-fourth of the polyprotein by the host signal peptidase and signal peptide peptidase (36, 43, 44), resulting in the maturation of capsid protein, two envelope proteins, and viroporin p7. The nonstructural protein 2 (NS2) protease cleaves its own carboxyl terminus, and then NS3 cleaves the appropriate downstream positions to produce NS3, NS4A, NS4B, NS5A, and NS5B (24, 60), which form the replication complex, together with several host proteins (14, 35).

NS5A is a membrane-anchored zinc-binding phosphoprotein that appears to possess diverse functions, including the suppression of host defense and the regulation of virus replication (1, 15, 58), but its biological function remains unclear. Several groups, including ours, have suggested that the molecular chaperone, heat shock protein 90 (Hsp90), and several cochaperones participate in the replication complex of HCV through interaction with NS5A or other NS proteins (45, 56, 65). Hsp90 is the highly conserved and ubiquitously expressed protein that acts as a key regulator for the turnover and the activities of more than 200 signaling proteins, including steroid receptors and cell-signaling kinases (66). The chaperone activity of Hsp90 contributes to the refolding of an unfolded protein in an ATP-dependent manner, and the execution of Hsp90-dependent protein folding requires the formation of a multichaperone complex containing other chaperones (e.g., Hsp70, Hsp104, and Hsp40) and cochaperones (e.g., p23, Hop, and immunophilins) (4, 18, 48). Geldanamycin or its derivatives, which are represented as specific inhibitors of Hsp90, can destabilize and then degrade client proteins (41, 55).

The host chaperone mechanism is involved in the folding of viral polymerase to support viral replication (6, 27). Moreover, host chaperones have been reported to play roles in the assembly of viral particles and the sorting of virus proteins (9, 32, 38). We have previously reported that Hsp90 chaperone activities and chaperone-associated proteins are required for the efficient propagation of HCV (45, 56) and that human butyrate-induced transcript 1 (hB-ind1) is involved in the propagation of HCV through interactions with NS5A and Hsp90 via the coiled-coil domain and the FXXW motif, respectively (56). hB-ind1 was first reported to be a multiple-membrane-spanning protein consisting of 362 amino acids that possesses a significant homology with a cochaperones, p23, that regulates

* Corresponding author. Mailing address: Department of Molecular Virology, Research Institute for Microbial Diseases, Osaka University, 3-1, Yamadaoka, Suita-shi, Osaka 565-0871, Japan. Phone: 81-6-6879-8340. Fax: 81-6-6879-8269. E-mail: matsuura@biken.osaka-u.ac.jp.

▽ Published ahead of print on 5 August 2009.

Hsp90 function by its cochaperone activity (11). However, the roles of hB-ind1 in the life cycle of HCV have not been precisely clarified. In this study, we investigated the role of the Hsp90-related chaperone system, including hB-ind1, in the regulation of the RNA replication and particle production of HCV.

MATERIALS AND METHODS

Plasmids. The plasmids encoding hB-ind1, NS5A, Hsp90, and FK506-binding protein 8 (FKBP8) were prepared by methods described previously (45, 56). The DNA fragments encoding hB-ind1 mutants were prepared by PCR with the introduction of a silent mutation that is resistant to the short hairpin RNA in the hB-ind1 knockdown cells, as described previously (56). The human p23 gene and glucose-regulated protein 78 (GRP78) promoter region (−151 to +22) were amplified by PCR from the total cDNA and genomic DNA of Huh7 cells, respectively. The DNA fragments encoding mutants of hB-ind1 and p23 were prepared by the method of splicing by overlap extension (26) and introduced into pEF FLAGGs pGKpuro (28). The GRP78 promoter region was introduced between the KpnI and HindIII sites of pGL3-basic (Promega, Madison, WI) and designated pGRP78-luc. The reporter plasmid carrying a firefly luciferase gene under the control of the GR promoter (pGR-luc) was purchased from Panomics (Fremont, CA). The internal-control plasmid encoding a *Renilla* luciferase (pRL-TK) was purchased from Promega. The plasmid pFK-I_{389} neo/NS3-3′/NK5.1 (47) was kindly provided by R. Bartenschlager. The plasmids used in this study were confirmed by sequencing them with an ABI Prism 3130 genetic analyzer (Applied Biosystems, Tokyo, Japan).

Cells and virus infection. All cell lines were cultured at 37°C under a humidified atmosphere and 5% CO_2. The human embryonic kidney 293T and hepatocellular carcinoma Huh7 cell lines were maintained in Dulbecco's modified Eagle's medium (DMEM) (Sigma, St. Louis, MO) supplemented with 100 U/ml penicillin, 100 μg/ml streptomycin, and 10% fetal calf serum (FCS). The human hepatocellular carcinoma cell line Huh7.5.1 was kindly provided by F. Chisari (70) and was maintained in DMEM containing nonessential amino acids, 100 U/ml penicillin, 100 μg/ml streptomycin, and 10% FCS. The Huh9-13 cell line, which is a Huh7 cell line harboring a subgenomic HCV RNA replicon (35), was maintained in DMEM containing 10% FCS, nonessential amino acids, and 1 mg/ml G418 (Nakalai Tesque, Kyoto, Japan). The hB-ind1 knockdown cell line Huh-KD and control cell line Huh-ctrl were described previously (56). Huh-KD cells were transfected with each of the expression plasmids encoding wild-type or mutant hB-ind1 and cultured for 1 week in the presence of 10 μg/ml of puromycin. The remaining cells were used for the experiments described below. The viral RNA of JFH1 was introduced into Huh7.5.1 cells according to the method of Wakita et al. (62) for preparation of the infectious HCV particles in cell culture.

Antibodies. The rabbit anti-hB-ind1 antibody was prepared as described previously (56). Mouse monoclonal antibodies to HCV NS5A, influenza virus hemagglutinin (HA) and FLAG tags, and β-actin were purchased from Austral Biologicals (San Ramon, CA), Covance (Richmond, CA), and Sigma, respectively. Mouse anti-protein disulfide isomerase (PDI) immunoglobulin G2a (IgG2a) was from Affinity Bioreagents (Golden, CO). Mouse anti-double-stranded RNA (dsRNA) IgG2a (J1 and K2) antibodies were from Biocenter Ltd. (Szirak, Hungary). Alexa Fluor 488 (AF488)-conjugated anti-mouse IgG1, AF647-conjugated anti-rabbit IgG, and AF594-conjugated anti-mouse IgG2a and IgG2b antibodies were from Invitrogen (San Diego, CA).

Transfection, immunoblotting, and immunoprecipitation. Transfection and immunoprecipitation analyses were carried out as described previously (25, 45). Immunoprecipitates boiled in loading buffer were subjected to 12.5% sodium dodecyl sulfate-polyacrylamide gel electrophoresis. The proteins were transferred to polyvinylidene difluoride membranes (Millipore, Bedford, MA) and were reacted with the appropriate antibodies. The immune complexes were visualized with Super Signal West Femto substrate (Pierce, Rockford, IL) and detected by an LAS-3000 image analyzer system (Fujifilm, Tokyo, Japan). The protein bands of GRP78 and β-actin were quantified by Multi Gauge software (Fujifilm), and the values of GRP78 expression were normalized with those of β-actin.

Quantitative reverse transcriptase PCR. HCV RNA was estimated by the method described previously (56). Total RNA was prepared from cells by using an RNeasy minikit (Qiagen, Tokyo, Japan). First-strand cDNA was synthesized using an RNA LA PCR in vitro cloning kit (Takara Bio Inc., Shiga, Japan) and random primers. Each cDNA was estimated with Platinum SYBR green qPCR SuperMix UDG (Invitrogen) according to the manufacturer's protocol. Fluorescent signals were analyzed with an ABI Prism 7000 (Applied Biosystems). The internal ribosomal entry site regions of HCV and mRNAs of GAPDH (glyceraldehyde-3-phosphate dehydrogenase), GRP78, and growth arrest- and DNA damage-inducible gene 153 (GADD153) were amplified using the primer pairs 5′-GAGTGTCGTGCAGCCTCCA-3′ and 5′-CACTCGCAAGCACCCTATCA-3′, 5′-GAAGGTGAAGGTCGGAGTC-3′ and 5′-GAAGGTGAAGGTCGGAGTC-3′, 5′-CGCCAAGCGGCTCATC-3′ and 5′-AACCACCTTGAACGGCAAGA-3′, and 5′-AGCTGGAACCTGAGGAGAGA-3′ and 5′-TGGATCAGTCTGGAAAAGCA-3′, respectively. The values of the HCV genome or each mRNA were normalized with those of GAPDH mRNA. Each PCR product was detected as a single band of the correct size on agarose gel electrophoresis (data not shown).

In vitro transcription and RNA transfection. The plasmid pFK-I_{389} neo/NS3-3′/NK5.1 was linearized by treatment with ScaI and then transcribed in vitro using the MEGAscript T7 kit (Applied Biosystems) according to the manufacturer's protocol. The in vitro-transcribed RNA was electroporated into cells at 4 million cells/0.4 ml under conditions of 270 V and 960 μF using a Gene Pulser (Bio-Rad, Hercules, CA). The colony formation assay was carried out by a method described previously (45).

Indirect immunofluorescence assay. Cells cultured on glass slides were fixed with 4% paraformaldehyde in phosphate-buffered saline (PBS) at room temperature for 30 min. After being washed twice with PBS, the cells were permeabilized for 20 min at room temperature with PBS containing 0.25% saponin and blocked with PBS containing 0.2% gelatin (gelatin-PBS) for 60 min at room temperature. The cells were incubated with gelatin-PBS containing rabbit anti-hB-ind1 antibody, mouse anti-NS5A IgG1, mouse anti-PDI IgG2a, mouse anti-FKBP8 IgG2b, or mouse anti-dsRNA IgG2a (J1 and K2) at 37°C for 60 min; washed three times with PBS containing 1% Tween 20; and incubated with gelatin-PBS containing AF488-conjugated anti-mouse IgG1 or AF647-conjugated anti-rabbit or AF594-conjugated anti-mouse IgG2a or IgG2b antibodies at 37°C for 60 min. Finally, the cells were washed three times with PBS containing 1% Tween 20 and observed with a FluoView FV1000 laser scanning confocal microscope (Olympus, Tokyo, Japan).

Correlative FM-EM. Correlative fluorescence microscopy-electron microscopy (FM-EM) allows individual cells to be examined both in an overview with FM and in a detailed subcellular-structure view with EM (51). The endogenous hB-ind1 and NS5A were stained and observed in the HCV replicon cells by the correlative FM-EM method as described previously (45).

Luciferase assay. Each plasmid was transfected into Huh7, Huh9-13, and interferon (IFN)-cured cells seeded in a 12-well plate, and the cells were treated with 1 μM dexamethasone (Sigma) for 12 h or with 17-dimethylamino-ethylamino-17-demethoxygeldanamycin (DMAG) (Sigma) for 6 h at 36 h posttransfection and lysed in 200 μl of passive lysis buffer (Promega). Luciferase activity was measured in 20-μl aliquots of the cell lysates using a Dual-Luciferase Reporter Assay System (Promega). Firefly luciferase activity was standardized with that of *Renilla* luciferase cotransfected with the internal-control plasmid pRL-TK. The resulting values were expressed as the increase in relative light units (RLU).

Statistical analysis. Results were expressed as the mean ± standard deviation. The significance of differences in the means was determined by Student's *t* test.

RESULTS

The p23-like domain of hB-ind1 has cochaperone activity. Although we had previously reported that hB-ind1 regulates HCV RNA replication through interaction with NS5A and Hsp90, the molecular mechanisms underlying the regulation of HCV replication remained to be clarified. To gain more insights into the potential cochaperone activity of hB-ind1 in the Hsp90 chaperone system, we prepared expression plasmids encoding a wild-type p23 and three p23 mutants—one in which the FXXW motif was replaced with AXXA (p23AxxA), one in which the cochaperone domain of p23 was replaced with the p23-like domain of hB-ind1 (cp23), and one in which both substitutions were made (cp23AxxA) (Fig. 1A). HA-tagged Hsp90 was coexpressed with FLAG-tagged p23 or the FLAG-tagged p23 mutants in 293T cells (Fig. 1B). Hsp90 was coimmunoprecipitated with wild-type p23 and a cp23 mutant, but not with the p23AxxA or cp23AxxA mutants, indicating that the FXXW motif of hB-ind1, as is the case with that of p23

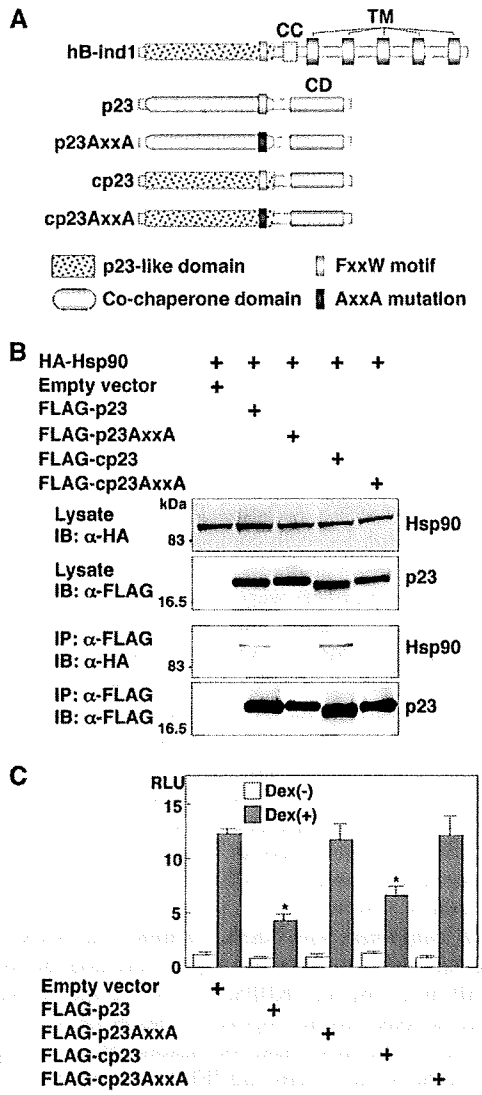

FIG. 1. Construction and characterization of p23 mutants. (A) Structures of hB-ind1, p23, and the three p23 mutants. hB-ind1 consists of a p23-like domain, an FXXW motif, a coiled-coil domain (CC), and a transmembrane domain (TM). p23 consists of a cochaperone domain, an FXXW motif, and a chaperone domain (CD). The three p23 mutants, p23AxxA, cp23, and cp23AxxA, were constructed by replacing the FXXW motif with AXXA, the cochaperone domain of p23 with the p23-like domain of hB-ind1, and both of the regions, respectively. (B) FLAG-tagged p23, p23AxxA, cp23, or cp23AxxA was coexpressed with HA-tagged Hsp90 in 293T cells and immunoprecipitated (IP) with anti-FLAG antibody. The immunoprecipitates were subjected to immunoblotting (IB). (C) The expression plasmid encoding FLAG-tagged p23, cp23, p23AxxA, or cp23AxxA was cotransfected with pGR-luc and pRL-TK plasmids into 293T cells and treated with 1 mM dexamethasone [Dex(+)] at 36 h posttransfection or untreated [Dex(−)], and the luciferase activities were determined at 12 h of incubation. The firefly luciferase activity was normalized with that of *Renilla* luciferase, and the GR-responsive promoter activity was indicated as the RLU. The error bars indicate standard deviations. The asterisks indicate significant differences ($P < 0.01$) versus the control value. The data shown are representative of three independent experiments.

(67), is also involved in binding to Hsp90. Hsp90 participates in the folding and stabilization of the ligand-binding domain of the glucocorticoid receptor (GR), together with p23 and other cofactors (49). p23 was shown to act not only in the activation (30), but also in the inhibition, of GR signaling (67). To examine whether hB-ind1 has the ability to work as a cochaperone in an Hsp90-dependent manner, each of the plasmids encoding p23 or the p23 mutants was cotransfected with a reporter plasmid carrying a firefly luciferase gene under the control of the GR promoter (pGR-luc), together with an internal-control plasmid (pRL-TK), and GR-mediated transcriptional activity was determined at 12 h after treatment with dexamethasone, a ligand of GR. Expression of the p23 or cp23 mutant, but not of the AXXA mutants, significantly inhibited GR-mediated transcription (Fig. 1C). These results indicate that the p23-like domain of hB-ind1 possesses cochaperone activity comparable to that of p23.

The p23-like domain of hB-ind1 is interchangeable with the p23 cochaperone domain during complex formation with NS5A, Hsp90, and FKBP8. Previous reports have suggested that HCV NS5A interacts with several host proteins, including FBL2 (63), vesicle-associated membrane protein-associated protein subtype A (VAP-A) (61), VAP-B (25), FKBP8 (45), and hB-ind1 (56), and that these interactions participate in the replication of HCV. We have shown that hB-ind1 interacts with NS5A and Hsp90 through the coiled-coil domain and the FXXW motif in the p23-like domain, respectively, and that coexpression of FKBP8 enhances the interaction of Hsp90 with hB-ind1 (56). To determine the effect of the mutation in the p23-like domain of hB-ind1 on interaction with Hsp90, NS5A, and FKBP8, we prepared an expression plasmid encoding wild-type hB-ind1 and three hB-ind1 mutants, one in which the p23-like domain was replaced with the cochaperone domain of p23 (chB-ind1), one in which the FXXW motif was replaced with AXXA (hB-ind1AxxA), and one in which both replacements were made (chB-ind1AxxA) (Fig. 2A). The FLAG-tagged wild-type or mutant hB-ind1 was coexpressed with HA-tagged Hsp90 (Fig. 2B, left) or HA-tagged NS5A (Fig. 2B, right) in 293T cells and immunoprecipitated with anti-FLAG antibody. Hsp90 was coprecipitated with wild-type hB-ind1 and the chB-ind1 mutant, but not with the hB-ind1AXXA and chB-ind1AXXA mutants (Fig. 2B, left), confirming that the FXXW motif is crucial for the interaction with Hsp90. In contrast, NS5A was coprecipitated with each of the hB-ind1 proteins, suggesting that mutation in the p23-like domain of hB-ind1 has no effect on the binding of hB-ind1 to NS5A through the coiled-coil domain (Fig. 2B, right). To determine the effect of FKBP8 expression on the interaction between hB-ind1 and Hsp90, FLAG-tagged wild-type hB-ind1 or the chB-ind1 mutant was coexpressed with HA-tagged FKBP8 and/or Hsp90 in 293T cells and immunoprecipitated with anti-FLAG antibody. The amounts of Hsp90 coprecipitated with hB-ind1 or chB-ind1 were increased by coexpression of FKBP8 (Fig. 2C). To further examine the interaction of hB-ind1 with Hsp90 and NS5A at an endogenous expression level in Huh9-13 cells harboring an HCV subgenomic RNA replicon, lysates of the replicon cells were subjected to immunoprecipitation analysis. Endogenous Hsp90 and NS5A were specifically coimmunoprecipitated with endogenous hB-ind1 (Fig. 2D). These results suggest that the p23-like domain of hB-ind1 is inter-

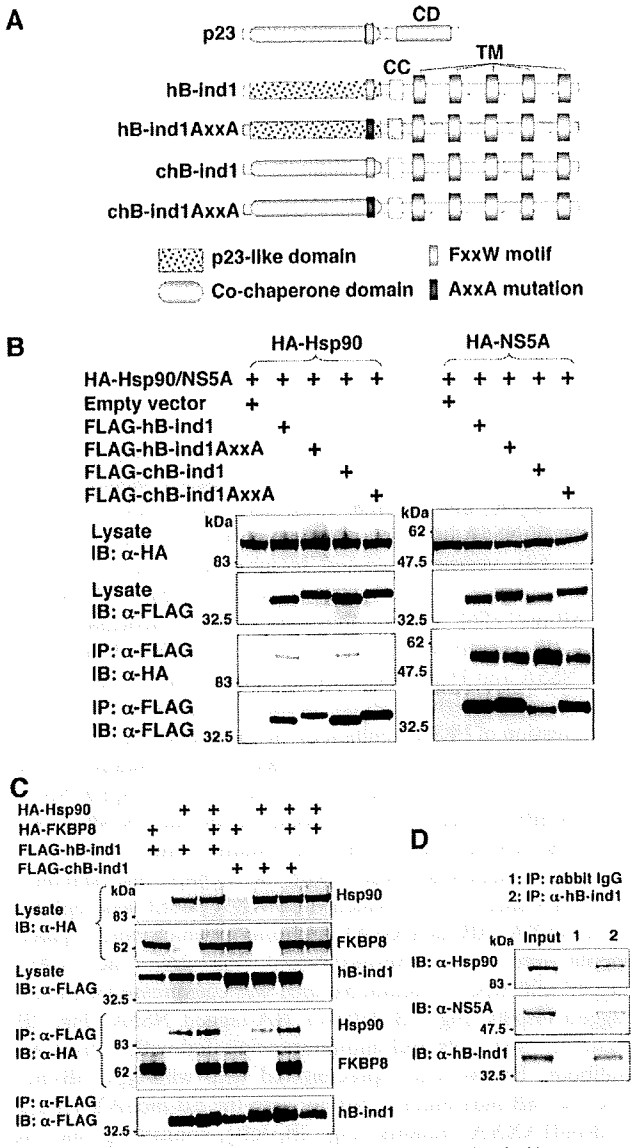

FIG. 2. Construction and characterization of hB-ind1 mutants. (A) Structures of p23, hB-ind1, and the three hB-ind1 mutants. The three hB-ind1 mutants, hB-ind1AxxA, chB-ind1, and chB-ind1AxxA, were constructed by replacing the FXXW motif with AXXA, the p23-like domain of hB-ind1 with the cochaperone domain of p23, and both of the regions, respectively. (B) FLAG-tagged hB-ind1, hB-ind1 AxxA, chB-ind1, or chB-ind1AxxA was coexpressed with either HA-tagged Hsp90 (left) or NS5A (right) in 293T cells and immunoprecipitated (IP) with anti-FLAG antibody. The immunoprecipitates were subjected to immunoblotting (IB). (C) HA-tagged Hsp90 and HA-FKBP8 were expressed with FLAG-tagged hB-ind1 and chB-ind1 in various combinations in 293T cells and immunoprecipitated with anti-FLAG antibody, and the immunoprecipitates were detected by immunoblotting. (D) Endogenous hB-ind1 in Huh9-13 cells harboring subgenomic HCV replicon RNA was immunoprecipitated with anti-hB-ind1 rabbit IgG (lane 2). The cell lysate was mixed with normal rabbit IgG as a negative control (lane 1). The immunoprecipitates were analyzed by immunoblotting with an antibody to Hsp90, NS5A, or hB-ind1. The data shown are representative of three independent experiments.

changeable with the cochaperone domain of p23 during complex formation with NS5A, Hsp90, and FKBP8.

Cochaperone activity in the p23-like domain of hB-ind1 is required for propagation of HCV. The p23-like domain of hB-ind1 has been suggested to be required for HCV propagation (56). However, the involvement of the cochaperone activity of hB-ind1 in HCV propagation has not been examined. To assess the effect of cochaperone activity in the p23-like domain of hB-ind1 on the RNA replication and particle production of HCV, each of the expression plasmids encoding the FLAG-tagged wild-type or mutant hB-ind1 carrying the silent mutations resistant to small interfering RNA was transfected into hB-ind1 knockdown (Huh-KD) cells and cultured for a week in the presence of puromycin. The expressions of FLAG-tagged hB-ind1 and the mutants in the Huh-KD cells were comparable to that of the endogenous hB-ind1 in the control (Huh-ctrl) cells transfected with an empty vector (Fig. 3A). Subgenomic HCV replicon RNA transcribed from pFK-I_{389} neo/NS3-3′/NK5.1 was transfected into these cells and cultured for 4 weeks in the presence of G418. Although the number of colonies was reduced in the Huh-KD cells compared with the Huh-ctrl cells after transfection with an empty vector, as described previously (56), the colony numbers were recovered by the expression of the hB-ind1 or chB-ind1 mutant, but not by that of the hB-ind1AXXA or chB-ind1AXXA mutants (Fig. 3B). Similarly, intracellular HCV RNA and infectious viral titers in the culture supernatants of Huh-KD cells infected with JFH1 virus were partially recovered by the expression of the hB-ind1 or chB-ind1 mutant, but not by that of the hB-ind1AXXA or chB-ind1AXXA mutant (Fig. 3C). These results suggest that cochaperone activity in the p23-like domain of hB-ind1 is required for HCV propagation and that the cochaperone domain of p23 can substitute for the p23-like domain of hB-ind1.

hB-ind1 colocalizes with NS5A, FKBP8, and dsRNA on the membranous web. Our previous report revealed the interplay among hB-ind1, Hsp90, FKBP8, and NS5A and showed that these interactions play an important role in HCV replication (56). However, the subcellular localization of the endogenous hB-ind1 in the replicon cells and JFH1 virus-infected cells has not been precisely assessed. To determine the subcellular localization of hB-ind1 in the context of HCV replication, the expression of hB-ind1 and NS5A in the replicon cells and JFH1 virus-infected cells was examined by immunofluorescence analyses (Fig. 4A). Endogenous hB-ind1 was colocalized with the endoplasmic reticulum (ER)-marker PDI and NS5A as dot-like structures in the Huh9-13 replicon cells (Fig. 4A, top) and in cells infected with JFH1 virus (Fig. 4A, bottom), and these dot-like structures disappeared in concert with the loss of NS5A expression by treatment with IFN-α in the replicon cells and was not observed in the mock-infected Huh7.5.1 cells. Furthermore, FKBP8 (Fig. 4B, top) and dsRNA (Fig. 4B, bottom) were colocalized with hB-ind1 and NS5A in the dot-like structures in Huh9-13 replicon cells. These results indicate that HCV replicating RNA is localized with hB-ind1, FKBP8, and NS5A in the dot-like compartments. HCV RNA replication or expression of viral proteins leads to formation of the convoluted membranous structures designated the membranous web (14, 23). The large structures of the replication complexes in the replicon cells indicate membranous webs with

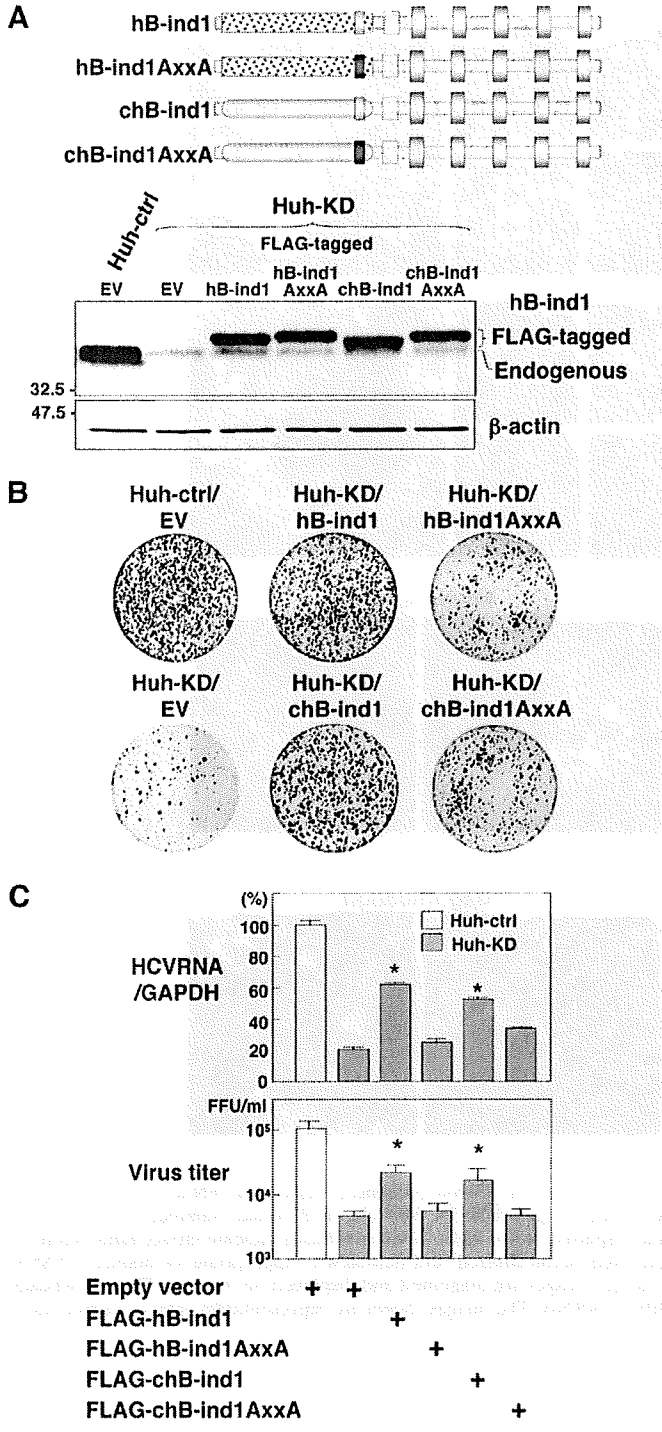

FIG. 3. Effects of the cochaperone activity of hB-ind1 on the propagation of HCV. (A) Huh-KD cells were transfected with either an empty vector or an expression plasmid encoding FLAG-tagged hB-ind1, hB-ind1AxxA, chB-ind1, or chB-ind1AxxA, which are resistant to small interfering RNA due to the introduction of silent mutations, and cultured for a week in the presence of 10 μg/ml of puromycin. The surviving cells were used in the subsequent experiments. The endogenous and exogenous expression of hB-ind1 and the mutants was detected by immunoblotting. The control cell line (Huh-ctrl) or the Huh-KD cell line transfected with an empty vector (EV) was used as a control. (B) Huh-KD cells were transfected with the plasmids and then selected with puromycin. The resulting cells were further transfected with a replicon RNA transcribed from pFK-I_{389} neo/NS3-3′/NK5.1, cultured for 4 weeks in the presence of 1 mg/ml of G418, and stained with crystal violet after fixation with 4% paraformaldehyde. The Huh-KD cell line transfected with an empty vector (EV) was used as a positive control. (C) The cells prepared as described above were infected with JFH1 virus and harvested at 3 days postinfection. The amount of intracellular HCV RNA was estimated by quantitative reverse transcriptase PCR and normalized with that of GAPDH mRNA. The values of HCV RNA are presented as percentages versus those of Huh-ctrl cells transfected with an empty vector. The culture supernatants were subjected to a focus-forming assay. Virus titers are presented as focus-forming units (FFU) per ml. The error bars indicate standard deviations. The asterisks indicate significant differences ($P < 0.01$) versus the value of the control. The data shown are representative of three independent experiments.

restricted motility (68). To further analyze the subcellular compartments, including hB-ind1 and NS5A, the same field of the Huh9-13 replicon cells was observed under FM and EM by using the correlative FM-EM technique (Fig. 5A, upper two rows). The large structures that included hB-ind1 and NS5A in the replicon cells were observed under FM and EM (white-boxed areas) and further magnified (black-boxed areas). Convoluted membranous structures that consisted of small vesicles and that were similar to the membranous web were observed. Another field of view yielded similar results (Fig. 5A, lower two rows). The membranous web resembling the convoluted structures was not observed in the Huh9-13 cells depleted of viral RNA by IFN treatment (Fig. 5B). Together, these results suggest that hB-ind1 interacts with NS5A on the membranous web in cells replicating HCV RNA.

Hsp90 is involved in the circumvention of the UPR during HCV replication. Hsp90 regulates the folding and stability of proteins in all eukaryotes (59), and inhibition of the chaperone pathway suppresses correct protein folding, which leads to induction of proteasome-mediated degradation of the unfolded proteins and the unfolded protein response (UPR). Our previous (46) and present studies (Fig. 4 and 5) showed that several cochaperone components are recruited in the membranous web, suggesting that the Hsp90 chaperone system participates in the replication complex to circumvent the induction of the UPR and to maintain the folding of the host and viral proteins in a replication-competent state. To determine the induction of the UPR by HCV replication, Huh9-13 replicon cells were transfected with a reporter plasmid carrying a firefly luciferase gene under the control of the GRP78 promoter, which is activated by the induction of the UPR, together with an internal-control plasmid. Although the GRP78 promoter activity was slightly enhanced in the Huh9-13 cells compared to that in the parental cells, a fourfold increase of GRP78 promoter activity in the replicon cells was observed after treatment with an Hsp90 inhibitor, DMAG, in contrast to the twofold increase in similarly treated parental Huh7 cells, and the activation of the GRP78 promoter was canceled by treatment with IFN-α despite DMAG treatment (Fig. 6A), suggesting that the Hsp90 chaperone system participates in the circumvention of the UPR induced by the replication of HCV RNA. In addition, activation of GRP78 at transcriptional and translational levels after treatment with DMAG was higher in the

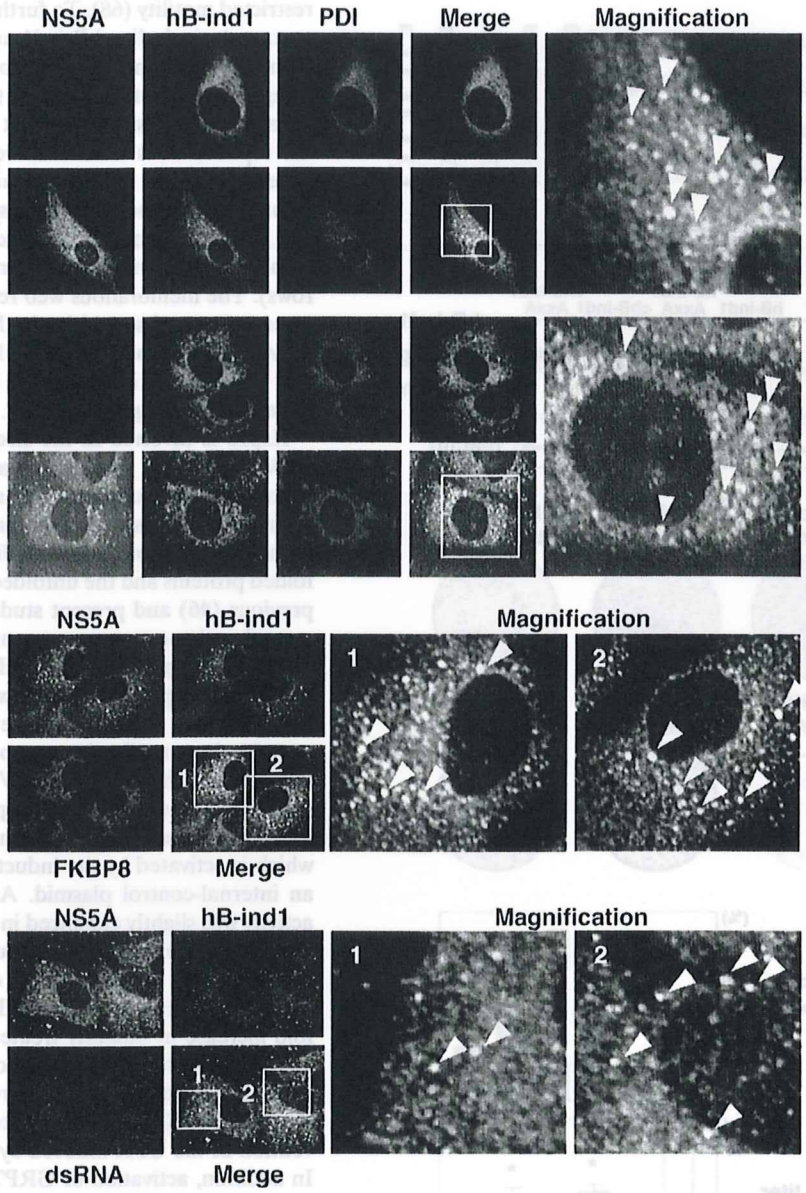

FIG. 4. Intracellular localization of hB-ind1 in replicon cells and infected cells. (A) Huh9-13 replicon cells with IFN-α or untreated and Huh7.5.1 cells infected with JFH1 virus or naïve cells were stained with antibodies against NS5A, hB-ind1, or PDI and examined by immunofluorescence assay. The boxed areas in the merged images are magnified and displayed on the right. The arrowheads indicate intracellular positions colocalized with NS5A, hB-ind1, and PDI. (B) Huh9-13 replicon cells were fixed, permeabilized, and stained with appropriate antibodies to NS5A, hB-ind1, and FKBP8 (top) or dsRNA (bottom). The boxed areas in the merged images are magnified and displayed on the right. The arrowheads indicate intracellular positions colocalized with NS5A, hB-ind, and FKBP8 or dsRNA. The images shown are representative of three independent experiments.

HCV replicon cells than in the parental cells or in cured cells, which were depleted of HCV RNA by treatment with IFN-α (Fig. 6B). Furthermore, DMAG treatment enhanced the transcription of the UPR marker protein GADD153 at a higher level in the replicon cells than in the parental Huh7 or the cured cells (Fig. 6C). These results suggest that the Hsp90-dependent chaperone system plays a crucial role in the folding of the host and viral proteins involved in HCV replication and in the regulation of UPR induction.

DISCUSSION

Studies of the relationship between Hsp90 and steroid receptors, such as GR, have revealed the activities of cochaperones (52, 67). Cochaperones, such as p23, appear to interact with and dissociate from Hsp90 and the client protein complex in a defined order. These cochaperones participate in the chaperone complex in a late step and promote the dissociation of the client proteins from Hsp90 to facilitate formation of the

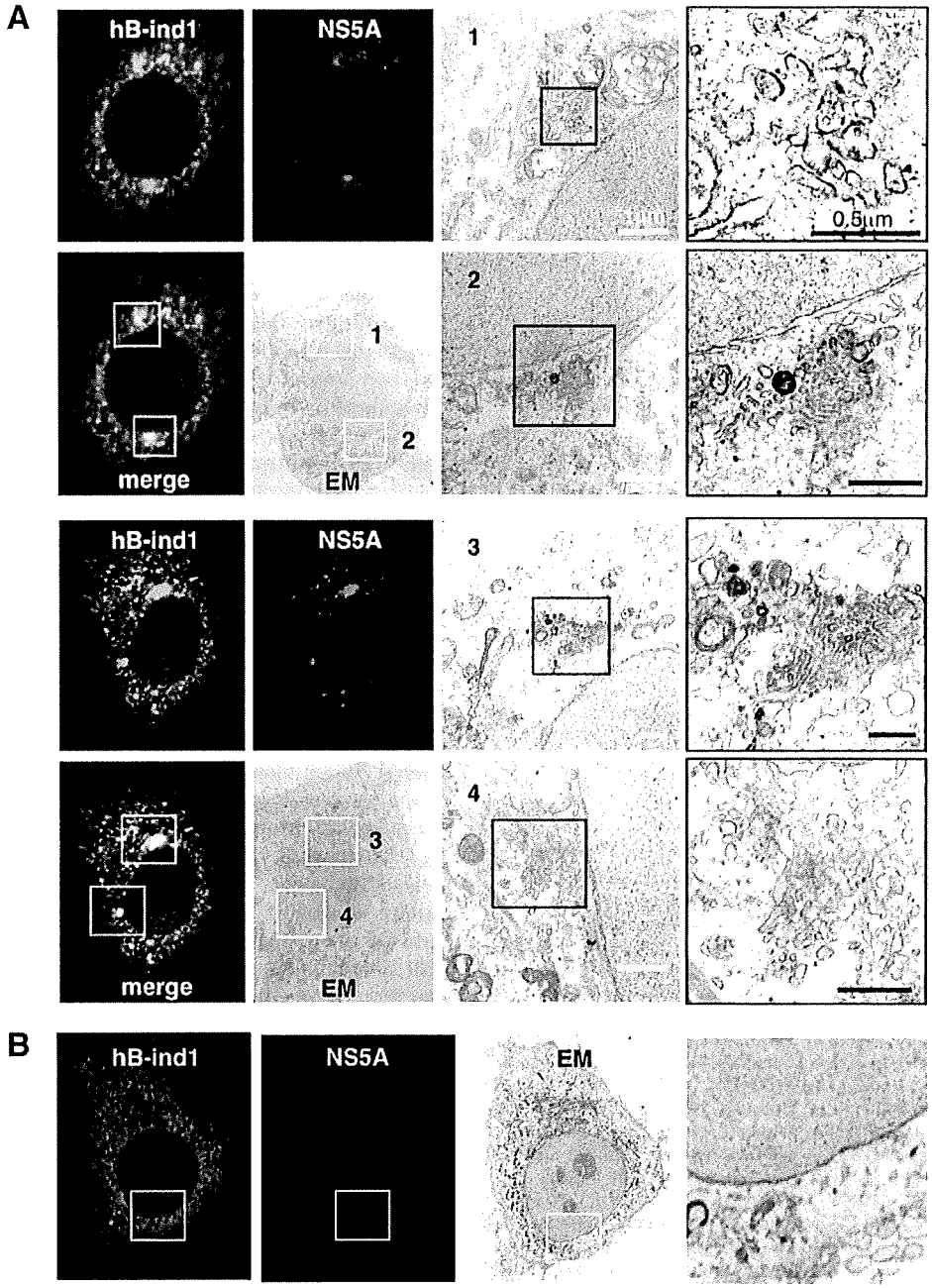

FIG. 5. hB-ind1 interacts with NS5A in the membranous web. Huh9-13 replicon cells were stained with specific antibodies to hB-ind1 and NS5A. Identical fields of Huh9-13 (A) or the cured cells (B) were observed under EM by using the correlative FM-EM technique. The white-boxed areas indicate the colocalized areas of hB-ind1 with NS5A. Magnified views of the white-boxed areas are displayed in the third column from the left. The right column contains further-magnified images of each of the black-boxed areas. Another field of view is presented in the lower two rows.

chaperone complex in the next chaperone cycle (16–18). In this study, we have shown that hB-ind1 participates in HCV replication and that the p23-like domain of hB-ind1 possesses cochaperone activity comparable to that of the cochaperone domain of p23, suggesting that hB-ind1 is involved in the recycling of the chaperone complex in the membranous web to maintain the function of the replication complex of HCV.

Previous studies have indicated that HCV proteins rearrange the ER membrane into the small convoluted membranous vesicles that are collectively known as the membranous web, and these vesicles have been suggested to be the intracellular compartments in which HCV replication takes place (14, 23, 68). In the living replicon cells, two forms of replication complexes, small and large vesicles, are detected, both of which include the viral replication complexes (68). Large vesicles, corresponding to membranous webs, exhibit restricted motil-

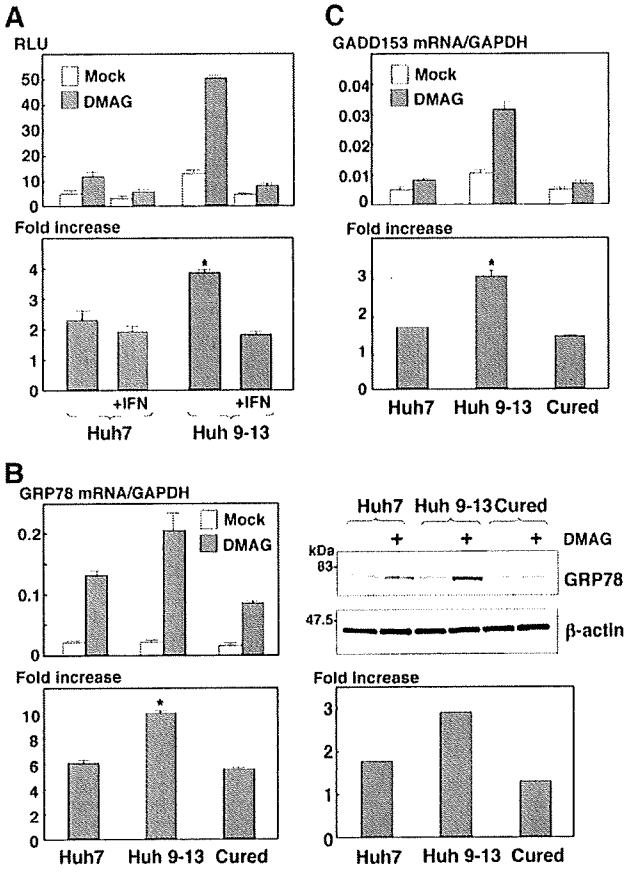

FIG. 6. Effect of Hsp90 inhibitor on the induction of the UPR in HCV replicon cells. (A) Huh7 and Huh9-13 replicon cells were transfected with a reporter plasmid, pGRP78-luc, and an internal-control plasmid, pRL-TK. The transfected cells were treated with IFN-α (+IFN) from 6 to 36 h posttransfection or left untreated and then further incubated for 6 h in the presence or absence of 1 μM DMAG. The resulting cells were harvested and subjected to a dual-luciferase assay. The firefly luciferase activity is indicated as the RLU (top) after standardization with that of *Renilla* luciferase. The enhancement of promoter activity by treatment with DMAG is presented as the increase (bottom). (B) Huh7 cells, Huh9-13 cells, and Huh9-13 cells cured by IFN-α treatment (Cured) were cultured for 6 h in the presence or absence of 1 μM DMAG, and the amount of GRP78 mRNA was measured by real-time PCR. The value of the mRNA was normalized with the amount of GAPDH mRNA (upper left), and the transcriptional enhancement by treatment with DMAG is presented as the increase (lower left). The expression levels of GRP78 and β-actin in the cells were determined by immunoblotting (upper right) and are presented as the increase (lower right). (C) The amounts of GADD153 mRNA in Huh7 cells, Huh9-13 cells, and the cured cells cultured for 6 h in the presence or absence of 1 μM DMAG were measured by real-time PCR. The values of the mRNA were normalized with the amount of GAPDH mRNA (top), and the transcriptional enhancement by treatment with DMAG is presented as the increase (bottom). The error bars indicate standard deviations. The asterisks indicate significant differences ($P < 0.01$) versus the control value. The data shown are representative of three independent experiments.

ity, while small vesicles show fast movement (68), and FM and EM have revealed that NS5A is colocalized with hB-ind1, as well as FKBP8 (45), in the membranous webs. hB-ind1 was first identified as a regulator of Rac1 that activates JNK and NF-κB (11). Rac1 is a member of the Rho GTPase family and plays crucial roles in cytoskeletal dynamics, membrane ruffling, and gene transcription through the effectors of the Rho GTPase family members. IQGAP1 and PAK1 are Rac1 effectors that bind to Rac proteins and are also involved in the replication of HCV (5, 7, 19, 31, 50). The tetratricopeptide repeat domain of immunophilin family members, such as FKBP8, has been shown to interact with Hsp90 (12, 45) and the GR-Hsp90 complex that leads to association with dynein for retrograde transport, along with microtubules (12). Hsp90 has been shown to play an important role in the interaction of transcriptase with genomic RNA of hepatitis B virus (27) and the nuclear transportation of the polymerase of influenza virus (40). Flock house virus also recruits Hsp90 in the polymerase synthesis in the early step of infection (9). Hsp90 may be involved in the regulation of the movement and arrangement of the HCV replication complexes through interaction with Rac1, hB-ind1, and FKBP8. Further investigation is needed to clarify the role of the Hsp90 chaperone system in the life cycle of HCV.

The surrounding membranes, including the membranous web, may protect the viral replication complex and RNA genome against digestion by the host proteases and nucleases (69). The replication complex is composed of viral nonstructural proteins and host proteins, including chaperone and cochaperone proteins. HCV NS5A has been shown to interact with various host proteins, including cochaperones, such as FKBP8 and hB-ind1, and to recruit a chaperone, Hsp90, into the replication complex through interaction with these cochaperones. Recruitment of the chaperone complex into the replication complex is crucial for the correct folding of newly synthesized viral proteins to maintain the efficient replication of the viral genome. HCV replication has been shown to be improved by the adaptive mutations suppressing the phosphorylation status of NS5A in the replicon cells (3). Although suppression of the hyperphosphorylation of NS5A by treatment with kinase inhibitors improves the replication of the replicons that have no adaptive mutations (42), several kinase inhibitors have been shown to suppress the replication of the HCV replicon carrying the adaptive mutations (29), and phosphorylation of NS5A by casein kinase II was shown to improve virus production but not HCV RNA replication (57). Hsp90 is capable of directly modulating the activities of several kinases (37, 53, 54), and thus, it might be feasible that cochaperones, including hB-ind1 and FKBP8, participate in the propagation of HCV by regulating the phosphorylation status of NS5A in cooperation with Hsp90.

The host chaperone system regulates the quality of client proteins, and impairment of the chaperone activity induces accumulation of misfolded proteins and affects the natural cellular function and viability (20, 21, 33). In this study, DMAG treatment induced a higher level of UPR in HCV replicon cells than in parental and cured cells, indicating that the Hsp90 chaperone system participates in the maintenance of correct folding of the viral and host proteins in the replication complex in the membranous web and in the circumvention of the UPR induced by HCV replication. Treatment with geldanamycin or its derivatives has been shown to inhibit GRP94, which is the Hsp90 paralog located in the ER (10), and to disrupt the ER chaperone pathway, leading to the induction of ER-associated protein degradation, transcriptional attenuation, and eventually induction of apoptosis (34). ER chaperones, such as

GRP94, may also participate in the correct folding of the viral and host proteins in the replication complex for efficient replication of the HCV genome.

Geldanamycin and its derivatives have been reported to remarkably inhibit poliovirus replication in vivo without any emergence of drug-resistant escape mutants (22), suggesting that an inhibitor of the chaperone system may be a promising candidate for the treatment of viral infectious diseases with low risk of the emergence of drug-resistant viruses. In addition, Hsp90 inhibitors exhibit anticancer activities through the suppression of various cell signals essential for cancer growth and the enhancement of radiation sensitivity (2, 8, 13). In conclusion, our data indicate that hB-ind1 is included within the HCV replication complex and regulates HCV RNA replication through its own cochaperone activity. Hsp90 and cochaperones, including hB-ind1 and FKBP8, which are required for efficient HCV replication, should be ideal targets for the treatment of chronic hepatitis C with a low frequency of emergence of drug-resistant breakthrough viruses.

ACKNOWLEDGMENTS

We thank H. Murase for her secretarial work. We also thank R. Bartenschlager, T. Wakita, and F. V. Chisari for providing the plasmids and cell lines.

This work was supported in part by grants-in-aid from the Ministry of Health, Labor, and Welfare; the Ministry of Education, Culture, Sports, Science, and Technology; the Global Center of Excellence Program; the Foundation for Biomedical Research and Innovation; and the Naito Foundation.

REFERENCES

1. **Abe, T., Y. Kaname, I. Hamamoto, Y. Tsuda, X. Wen, S. Taguwa, K. Moriishi, O. Takeuchi, T. Kawai, T. Kanto, N. Hayashi, S. Akira, and Y. Matsuura.** 2007. Hepatitis C virus nonstructural protein 5A modulates the toll-like receptor-MyD88-dependent signaling pathway in macrophage cell lines. J. Virol. **81**:8953–8966.
2. **Bisht, K. S., C. M. Bradbury, D. Mattson, A. Kaushal, A. Sowers, S. Markovina, K. L. Ortiz, L. K. Sieck, J. S. Isaacs, M. W. Brechbiel, J. B. Mitchell, L. M. Neckers, and D. Gius.** 2003. Geldanamycin and 17-allylamino-17-demethoxygeldanamycin potentiate the in vitro and in vivo radiation response of cervical tumor cells via the heat shock protein 90-mediated intracellular signaling and cytotoxicity. Cancer Res. **63**:8984–8995.
3. **Blight, K. J., A. A. Kolykhalov, and C. M. Rice.** 2000. Efficient initiation of HCV RNA replication in cell culture. Science **290**:1972–1974.
4. **Bohen, S. P., A. Kralli, and K. R. Yamamoto.** 1995. Hold 'em and fold 'em: chaperones and signal transduction. Science **268**:1303–1304.
5. **Bost, A. G., D. Venable, L. Liu, and B. A. Heinz.** 2003. Cytoskeletal requirements for hepatitis C virus (HCV) RNA synthesis in the HCV replicon cell culture system. J. Virol. **77**:4401–4408.
6. **Brown, G., H. W. Rixon, J. Steel, T. P. McDonald, A. R. Pitt, S. Graham, and R. J. Sugrue.** 2005. Evidence for an association between heat shock protein 70 and the respiratory syncytial virus polymerase complex within lipid-raft membranes during virus infection. Virology **338**:69–80.
7. **Bryan, B. A., D. Li, X. Wu, and M. Liu.** 2005. The Rho family of small GTPases: crucial regulators of skeletal myogenesis. Cell Mol. Life Sci. **62**: 1547–1555.
8. **Calderwood, S. K., M. A. Khaleque, D. B. Sawyer, and D. R. Ciocca.** 2006. Heat shock proteins in cancer: chaperones of tumorigenesis. Trends Biochem. Sci. **31**:164–172.
9. **Castorena, K. M., S. A. Weeks, K. A. Stapleford, A. M. Cadwallader, and D. J. Miller.** 2007. A functional heat shock protein 90 chaperone is essential for efficient flock house virus RNA polymerase synthesis in *Drosophila* cells. J. Virol. **81**:8412–8420.
10. **Chavany, C., E. Mimnaugh, P. Miller, R. Bitton, P. Nguyen, J. Trepel, L. Whitesell, R. Schnur, J. Moyer, and L. Neckers.** 1996. p185erbB2 binds to GRP94 in vivo. Dissociation of the p185erbB2/GRP94 heterocomplex by benzoquinone ansamycins precedes depletion of p185erbB2. J. Biol. Chem. **271**:4974–4977.
11. **Courilleau, D., E. Chastre, M. Sabbah, G. Redeuilh, A. Atfi, and J. Mester.** 2000. B-ind1, a novel mediator of Rac1 signaling cloned from sodium butyrate-treated fibroblasts. J. Biol. Chem. **275**:17344–17348.
12. **Davies, T. H., Y. M. Ning, and E. R. Sanchez.** 2002. A new first step in activation of steroid receptors: hormone-induced switching of FKBP51 and FKBP52 immunophilins. J. Biol. Chem. **277**:4597–4600.
13. **Didelot, C., D. Lanneau, M. Brunet, A. L. Joly, A. De Thonel, G. Chiosis, and C. Garrido.** 2007. Anti-cancer therapeutic approaches based on intracellular and extracellular heat shock proteins. Curr. Med. Chem. **14**:2839–2847.
14. **Egger, D., B. Wolk, R. Gosert, L. Bianchi, H. E. Blum, D. Moradpour, and K. Bienz.** 2002. Expression of hepatitis C virus proteins induces distinct membrane alterations including a candidate viral replication complex. J. Virol. **76**:5974–5984.
15. **Evans, M. J., C. M. Rice, and S. P. Goff.** 2004. Genetic interactions between hepatitis C virus replicons. J. Virol. **78**:12085–12089.
16. **Freeman, B. C., S. J. Felts, D. O. Toft, and K. R. Yamamoto.** 2000. The p23 molecular chaperones act at a late step in intracellular receptor action to differentially affect ligand efficacies. Genes Dev. **14**:422–434.
17. **Freeman, B. C., and K. R. Yamamoto.** 2002. Disassembly of transcriptional regulatory complexes by molecular chaperones. Science **296**:2232–2235.
18. **Frydman, J., and J. Hohfeld.** 1997. Chaperones get in touch: the Hip-Hop connection. Trends Biochem. Sci. **22**:87–92.
19. **Fukata, M., M. Nakagawa, and K. Kaibuchi.** 2003. Roles of Rho-family GTPases in cell polarisation and directional migration. Curr. Opin. Cell Biol. **15**:590–597.
20. **Garrido, C., M. Brunet, C. Didelot, Y. Zermati, E. Schmitt, and G. Kroemer.** 2006. Heat shock proteins 27 and 70: anti-apoptotic proteins with tumorigenic properties. Cell Cycle **5**:2592–2601.
21. **Garrido, C., S. Gurbuxani, L. Ravagnan, and G. Kroemer.** 2001. Heat shock proteins: endogenous modulators of apoptotic cell death. Biochem. Biophys. Res. Commun. **286**:433–442.
22. **Geller, R., M. Vignuzzi, R. Andino, and J. Frydman.** 2007. Evolutionary constraints on chaperone-mediated folding provide an antiviral approach refractory to development of drug resistance. Genes Dev. **21**:195–205.
23. **Gosert, R., D. Egger, V. Lohmann, R. Bartenschlager, H. E. Blum, K. Bienz, and D. Moradpour.** 2003. Identification of the hepatitis C virus RNA replication complex in Huh-7 cells harboring subgenomic replicons. J. Virol. **77**:5487–5492.
24. **Grakoui, A., D. W. McCourt, C. Wychowski, S. M. Feinstone, and C. M. Rice.** 1993. Characterization of the hepatitis C virus-encoded serine proteinase: determination of proteinase-dependent polyprotein cleavage sites. J. Virol. **67**:2832–2843.
25. **Hamamoto, I., Y. Nishimura, T. Okamoto, H. Aizaki, M. Liu, Y. Mori, T. Abe, T. Suzuki, M. M. Lai, T. Miyamura, K. Moriishi, and Y. Matsuura.** 2005. Human VAP-B is involved in hepatitis C virus replication through interaction with NS5A and NS5B. J. Virol. **79**:13473–13482.
26. **Ho, S. N., H. D. Hunt, R. M. Horton, J. K. Pullen, and L. R. Pease.** 1989. Site-directed mutagenesis by overlap extension using the polymerase chain reaction. Gene **77**:51–59.
27. **Hu, J., D. Flores, D. Toft, X. Wang, and D. Nguyen.** 2004. Requirement of heat shock protein 90 for human hepatitis B virus reverse transcriptase function. J. Virol. **78**:13122–13131.
28. **Huang, D. C., S. Cory, and A. Strasser.** 1997. Bcl-2, Bcl-XL and adenovirus protein E1B19kD are functionally equivalent in their ability to inhibit cell death. Oncogene **14**:405–414.
29. **Huang, Y., K. Staschke, R. De Francesco, and S. L. Tan.** 2007. Phosphorylation of hepatitis C virus NS5A nonstructural protein: a new paradigm for phosphorylation-dependent viral RNA replication? Virology **364**:1–9.
30. **Hutchison, K. A., L. F. Stancato, J. K. Owens-Grillo, J. L. Johnson, P. Krishna, D. O. Toft, and W. B. Pratt.** 1995. The 23-kDa acidic protein in reticulocyte lysate is the weakly bound component of the hsp foldosome that is required for assembly of the glucocorticoid receptor into a functional heterocomplex with hsp90. J. Biol. Chem. **270**:18841–18847.
31. **Ishida, H., K. Li, M. Yi, and S. M. Lemon.** 2007. p21-activated kinase 1 is activated through the mammalian target of rapamycin/p70 S6 kinase pathway and regulates the replication of hepatitis C virus in human hepatoma cells. J. Biol. Chem. **282**:11836–11848.
32. **Kampmueller, K. M., and D. J. Miller.** 2005. The cellular chaperone heat shock protein 90 facilitates Flock House virus RNA replication in *Drosophila* cells. J. Virol. **79**:6827–6837.
33. **Kim, H. P., D. Morse, and A. M. Choi.** 2006. Heat-shock proteins: new keys to the development of cytoprotective therapies. Exp. Opin. Ther. Targets **10**:759–769.
34. **Lai, E., T. Teodoro, and A. Volchuk.** 2007. Endoplasmic reticulum stress: signaling the unfolded protein response. Physiology **22**:193–201.
35. **Lohmann, V., F. Korner, J. Koch, U. Herian, L. Theilmann, and R. Bartenschlager.** 1999. Replication of subgenomic hepatitis C virus RNAs in a hepatoma cell line. Science **285**:110–113.
36. **McLauchlan, J., M. K. Lemberg, G. Hope, and B. Martoglio.** 2002. Intramembrane proteolysis promotes trafficking of hepatitis C virus core protein to lipid droplets. EMBO J. **21**:3980–3988.
37. **Miyata, Y., and I. Yahara.** 1992. The 90-kDa heat shock protein, HSP90, binds and protects casein kinase II from self-aggregation and enhances its kinase activity. J. Biol. Chem. **267**:7042–7047.
38. **Momose, F., T. Naito, K. Yano, S. Sugimoto, Y. Morikawa, and K. Nagata.**

2002. Identification of Hsp90 as a stimulatory host factor involved in influenza virus RNA synthesis. J. Biol. Chem. **277**:45306–45314.
39. **Moradpour, D., F. Penin, and C. M. Rice.** 2007. Replication of hepatitis C virus. Nat. Rev. Microbiol. **5**:453–463.
40. **Naito, T., F. Momose, A. Kawaguchi, and K. Nagata.** 2007. Involvement of Hsp90 in assembly and nuclear import of influenza virus RNA polymerase subunits. J. Virol. **81**:1339–1349.
41. **Neckers, L.** 2002. Hsp90 inhibitors as novel cancer chemotherapeutic agents. Trends Mol. Med. **8**:S55–S61.
42. **Neddermann, P., M. Quintavalle, C. Di Pietro, A. Clementi, M. Cerretani, S. Altamura, L. Bartholomew, and R. De Francesco.** 2004. Reduction of hepatitis C virus NS5A hyperphosphorylation by selective inhibition of cellular kinases activates viral RNA replication in cell culture. J. Virol. **78**:13306–13314.
43. **Okamoto, K., Y. Mori, Y. Komoda, T. Okamoto, M. Okochi, M. Takeda, T. Suzuki, K. Moriishi, and Y. Matsuura.** 2008. Intramembrane processing by signal peptide peptidase regulates the membrane localization of hepatitis C virus core protein and viral propagation. J. Virol. **82**:8349–8361.
44. **Okamoto, K., K. Moriishi, T. Miyamura, and Y. Matsuura.** 2004. Intramembrane proteolysis and endoplasmic reticulum retention of hepatitis C virus core protein. J. Virol. **78**:6370–6380.
45. **Okamoto, T., Y. Nishimura, T. Ichimura, K. Suzuki, T. Miyamura, T. Suzuki, K. Moriishi, and Y. Matsuura.** 2006. Hepatitis C virus RNA replication is regulated by FKBP8 and Hsp90. EMBO J. **25**:5015–5025.
46. **Okamoto, T., H. Omori, Y. Kaname, T. Abe, Y. Nishimura, T. Suzuki, T. Miyamura, T. Yoshimori, K. Moriishi, and Y. Matsuura.** 2008. A single-amino-acid mutation in hepatitis C virus NS5A disrupting FKBP8 interaction impairs viral replication. J. Virol. **82**:3480–3489.
47. **Pietschmann, T., V. Lohmann, A. Kaul, N. Krieger, G. Rinck, G. Rutter, D. Strand, and R. Bartenschlager.** 2002. Persistent and transient replication of full-length hepatitis C virus genomes in cell culture. J. Virol. **76**:4008–4021.
48. **Prapapanich, V., S. Chen, E. J. Toran, R. A. Rimerman, and D. F. Smith.** 1996. Mutational analysis of the hsp70-interacting protein Hip. Mol. Cell. Biol. **16**:6200–6207.
49. **Pratt, W. B., and D. O. Toft.** 1997. Steroid receptor interactions with heat shock protein and immunophilin chaperones. Endocr. Rev. **18**:306–360.
50. **Ridley, A. J., H. F. Paterson, C. L. Johnston, D. Diekmann, and A. Hall.** 1992. The small GTP-binding protein rac regulates growth factor-induced membrane ruffling. Cell **70**:401–410.
51. **Rieder, C. L., and S. S. Bowser.** 1985. Correlative immunofluorescence and electron microscopy on the same section of epon-embedded material. J. Histochem. Cytochem. **33**:165–171.
52. **Sanchez, E. R., D. O. Toft, M. J. Schlesinger, and W. B. Pratt.** 1985. Evidence that the 90-kDa phosphoprotein associated with the untransformed L-cell glucocorticoid receptor is a murine heat shock protein. J. Biol. Chem. **260**:12398–12401.
53. **Sato, S., N. Fujita, and T. Tsuruo.** 2000. Modulation of Akt kinase activity by binding to Hsp90. Proc. Natl. Acad. Sci. USA **97**:10832–10837.
54. **Stancato, L. F., A. M. Silverstein, J. K. Owens-Grillo, Y. H. Chow, R. Jove, and W. B. Pratt.** 1997. The hsp90-binding antibiotic geldanamycin decreases Raf levels and epidermal growth factor signaling without disrupting formation of signaling complexes or reducing the specific enzymatic activity of Raf kinase. J. Biol. Chem. **272**:4013–4020.
55. **Stravopodis, D. J., L. H. Margaritis, and G. E. Voutsinas.** 2007. Drug-mediated targeted disruption of multiple protein activities through functional inhibition of the Hsp90 chaperone complex. Curr. Med. Chem. **14**: 3122–3138.
56. **Taguwa, S., T. Okamoto, T. Abe, Y. Mori, T. Suzuki, K. Moriishi, and Y. Matsuura.** 2008. Human butyrate-induced transcript 1 interacts with hepatitis C virus NS5A and regulates viral replication. J. Virol. **82**:2631–2641.
57. **Tellinghuisen, T. L., K. L. Foss, and J. Treadaway.** 2008. Regulation of hepatitis C virion production via phosphorylation of the NS5A protein. PLoS Pathog. **4**:e1000032.
58. **Tellinghuisen, T. L., J. Marcotrigiano, and C. M. Rice.** 2005. Structure of the zinc-binding domain of an essential component of the hepatitis C virus replicase. Nature **435**:374–379.
59. **Terasawa, K., M. Minami, and Y. Minami.** 2005. Constantly updated knowledge of Hsp90. J. Biochem. **137**:443–447.
60. **Tomei, L., C. Failla, E. Santolini, R. De Francesco, and N. La Monica.** 1993. NS3 is a serine protease required for processing of hepatitis C virus polyprotein. J. Virol. **67**:4017–4026.
61. **Tu, H., L. Gao, S. T. Shi, D. R. Taylor, T. Yang, A. K. Mircheff, Y. Wen, A. E. Gorbalenya, S. B. Hwang, and M. M. Lai.** 1999. Hepatitis C virus RNA polymerase and NS5A complex with a SNARE-like protein. Virology **263**: 30–41.
62. **Wakita, T., T. Pietschmann, T. Kato, T. Date, M. Miyamoto, Z. Zhao, K. Murthy, A. Habermann, H. G. Krausslich, M. Mizokami, R. Bartenschlager, and T. J. Liang.** 2005. Production of infectious hepatitis C virus in tissue culture from a cloned viral genome. Nat. Med. **11**:791–796.
63. **Wang, C., M. Gale, Jr., B. C. Keller, H. Huang, M. S. Brown, J. L. Goldstein, and J. Ye.** 2005. Identification of FBL2 as a geranylgeranylated cellular protein required for hepatitis C virus RNA replication. Mol. Cell **18**:425–434.
64. **Wasley, A., and M. J. Alter.** 2000. Epidemiology of hepatitis C: geographic differences and temporal trends. Semin. Liver Dis. **20**:1–16.
65. **Watashi, K., N. Ishii, M. Hijikata, D. Inoue, T. Murata, Y. Miyanari, and K. Shimotohno.** 2005. Cyclophilin B is a functional regulator of hepatitis C virus RNA polymerase. Mol. Cell **19**:111–122.
66. **Whitesell, L., and S. L. Lindquist.** 2005. HSP90 and the chaperoning of cancer. Nat. Rev. Cancer. **5**:761–772.
67. **Wochnik, G. M., J. C. Young, U. Schmidt, F. Holsboer, F. U. Hartl, and T. Rein.** 2004. Inhibition of GR-mediated transcription by p23 requires interaction with Hsp90. FEBS Lett. **560**:35–38.
68. **Wolk, B., B. Buchele, D. Moradpour, and C. M. Rice.** 2008. A dynamic view of hepatitis C virus replication complexes. J. Virol. **82**:10519–10531.
69. **Yang, G., D. C. Pevear, M. S. Collett, S. Chunduru, D. C. Young, C. Benetatos, and R. Jordan.** 2004. Newly synthesized hepatitis C virus replicon RNA is protected from nuclease activity by a protease-sensitive factor(s). J. Virol. **78**:10202–10205.
70. **Zhong, J., P. Gastaminza, G. Cheng, S. Kapadia, T. Kato, D. R. Burton, S. F. Wieland, S. L. Uprichard, T. Wakita, and F. V. Chisari.** 2005. Robust hepatitis C virus infection in vitro. Proc. Natl. Acad. Sci. USA **102**:9294–9299.

ARTICLE

Journal of Cellular Biochemistry 106:1123–1135 (2009)

Identification of Annexin A1 as a Novel Substrate for E6AP-Mediated Ubiquitylation

Tetsu Shimoji,[1] Kyoko Murakami,[1] Yuichi Sugiyama,[1] Mami Matsuda,[1] Sachiko Inubushi,[2] Junichi Nasu,[1] Masayuki Shirakura,[1] Tetsuro Suzuki,[1] Takaji Wakita,[1] Tatsuya Kishino,[3] Hak Hotta,[2] Tatsuo Miyamura,[1] and Ikuo Shoji[1,2*]

[1]*Department of Virology II, National Institute of Infectious Diseases, Shinjuku-ku, Tokyo, Japan*

[2]*Division of Microbiology, Kobe University Graduate School of Medicine, Kobe, Hyogo, Japan*

[3]*Division of Functional Genomics, Center for Frontier Life Sciences, Nagasaki University, Nagasaki, Japan*

ABSTRACT

E6-associated protein (E6AP) is a cellular ubiquitin protein ligase that mediates ubiquitylation and degradation of p53 in conjunction with the high-risk human papillomavirus E6 proteins. However, the physiological functions of E6AP are poorly understood. To identify a novel biological function of E6AP, we screened for binding partners of E6AP using GST pull-down and mass spectrometry. Here we identified annexin A1, a member of the annexin superfamily, as an E6AP-binding protein. Ectopic expression of E6AP enhanced the degradation of annexin A1 in vivo. RNAi-mediated downregulation of endogenous E6AP increased the levels of endogenous annexin A1 protein. E6AP interacted with annexin A1 and induced its ubiquitylation in a Ca^{2+}-dependent manner. GST pull-down assay revealed that the annexin repeat domain III of annexin A1 is important for the E6AP binding. Taken together, our data suggest that annexin A1 is a novel substrate for E6AP-mediated ubiquitylation. Our findings raise the possibility that E6AP may play a role in controlling the diverse functions of annexin A1 through the ubiquitin-proteasome pathway. J. Cell. Biochem. 106: 1123–1135, 2009.

KEY WORDS: E6AP; ANNEXIN A1; UBIQUITIN; DEGRADATION

The ubiquitin/26S proteasome pathway plays important roles in the control of many basic cellular processes, such as cell cycle progression, signal transduction, transcriptional regulation, DNA repair, and the regulation of inflammation responses [Hershko and Ciechanover, 1998]. Ubiquitin is a 76-aa polypeptide that is highly conserved among eukaryotic organisms. The ubiquitin-proteasome pathway consists of an enzymatic cascade that ubiquitylates proteins, thereby targeting them for proteasomal degradation. The E1 ubiquitin-activating enzyme binds ubiquitin through a thioester linkage in an ATP-dependent manner [Ciechanover et al., 1981; Haas and Rose, 1982]. The activated ubiquitin is then transferred to the E2 ubiquitin-conjugating enzyme. E2 works in conjunction with the E3 ubiquitin-protein ligase, which is responsible for conferring substrate specificity [Hershko et al., 1986]. E3 mediates the transfer of ubiquitin to the target protein. The polyubiquitylated substrates are rapidly recognized and degraded by the 26S proteasome [Ciechanover, 1998; Ciechanover et al., 2000].

E6-associated protein (E6AP) was initially identified as the cellular factor that stimulates ubiquitin-dependent degradation of the tumor suppressor p53 in conjunction with the E6 protein of cervical cancer-associated human papillomavirus (HPV) types 16 and 18 [Huibregtse et al., 1993a; Scheffner et al., 1994]. The E6–E6AP complex functions as an E3 ubiquitin ligase in the ubiquitylation of p53 [Scheffner et al., 1993]. E6AP is the prototype of a family of ubiquitin ligases called HECT domain ubiquitin ligases, all of which contain a domain *h*omologous to the

Abbreviations used: E6AP, E6-associated protein; HPV, human papillomavirus; MALDI-TOF, matrix assisted laser desorption ionization-time of flight; MS, mass spectrometry; HCV, hepatitis C virus; MAb, monoclonal antibody; PAb, polyclonal antibody; GAPDH, glyceraldehydes-3-phosphate dehydrogenase; CHX, cycloheximide.

T. Shimoji and K. Murakami contributed equally to this work.

Grant sponsor: Japan Health Sciences Foundation; Grant sponsor: Ministry of Health, Labor, and Welfare; Grant sponsor: Promotion of Fundamental Studies in Health Sciences of the National Institute of Biomedical Innovation (NIBIO), Japan.

*Correspondence to: Ikuo Shoji, MD, PhD, Division of Microbiology, Kobe University Graduate School of Medicine, 7-5-1 Kusunoki-cho, Chuo-ku, Kobe, Hyogo 650-0017, Japan. E-mail: ishoji@med.kobe-u.ac.jp

Received 26 November 2008; Accepted 14 January 2009 • DOI 10.1002/jcb.22096 • 2009 Wiley-Liss, Inc.

Published online 9 February 2009 in Wiley InterScience (www.interscience.wiley.com).

E6AP carboxyl terminus [Huibregtse et al., 1995]. Known substrates of the E6–E6AP complex include the tumor suppressor p53 [Scheffner et al., 1993], the PDZ domain-containing protein scribble [Nakagawa and Huibregtse, 2000] and NFX1-91, a transcriptional repressor of the gene encoding hTERT [Gewin et al., 2004]. Interestingly, E6AP is not involved in the ubiquitylation of p53 in the absence of E6 [Talis et al., 1998]. Several potential E6-independent substrates for E6AP have been identified, such as HHR23A and HHR23B (the human orthologs of *Saccharomyces cerevisae* Rad23) [Kumar et al., 1999], Blk (a member of the Src family kinases) [Oda et al., 1999], Mcm7 (which is involved in DNA replication) [Kuhne and Banks, 1998], trihydrophobin 1 [Yang et al., 2007], and AIB1 (a steroid receptor coactivator) [Mani et al., 2006].

Some patients with Angelman syndrome, a severe neurological disorder linked to E6AP, have mutations within the catalytic cleft that have been shown to reduce E6AP ubiquitin ligase activity [Kishino et al., 1997; Cooper et al., 2004]. Despite the significant progress in the study of Angelman syndrome-associated E6AP mutations, none of the identified E6AP substrates have been directly linked to the disorder. The physiological functions of E6AP are poorly understood at present.

In an attempt to identify novel substrates of E6AP, we identified annexin A1 (formerly known as lipocortin 1) as an E6AP-binding protein. Annexin A1 is a 37-kDa member of the annexin superfamily of Ca^{2+} and phospholipid-binding proteins [Lim and Pervaiz, 2007]. Annexin A1 is involved in the inhibition of cell proliferation, anti-inflammatory effects, and the regulation of cell differentiation. In addition, annexin A1 is involved in the regulation of cell death signaling, phagocytosis of apoptosis, and the process of carcinogenesis [Buckingham et al., 2006; Lim and Pervaiz, 2007]. Annexin A1 is phosphorylated by various kinases such as tyrosine kinase, pp60c-src [Varticovski et al., 1988], protein kinase C [Oudinet et al., 1993], epidermal growth factor receptor protein kinase [Haigler et al., 1987], and hepatocyte growth factor receptor kinase [Skouteris and Schroder, 1996].

In this study, we have examined the possibility that the stability of annexin A1 is regulated through E6AP-dependent ubiquitylation. Our study revealed that E6AP mediates ubiquitin-dependent degradation of annexin A1 in a Ca^{2+}-dependent manner. Our results raise the possibility that E6AP may have a role in controlling the diverse functions of annexin A1.

MATERIALS AND METHODS

CELL CULTURE AND TRANSFECTION

Human embryonic kidney (HEK) 293T cells, and human cervical carcinoma C33-A cells were cultured in Dulbecco's modified Eagle's medium (DMEM) (Sigma, St. Louis, MO) supplemented with 50 IU/ml penicillin, 50 μg/ml streptomycin (Invitrogen, Carlsbad, CA), and 10% (v/v) fetal bovine serum (FBS) (JRH Biosciences, Lenexa, KS) at 37°C in a 5% CO_2 incubator. HEK 293T cells and C33-A cells were transfected with plasmid DNA using FuGene 6 transfection reagents (Roche, Mannheim, Germany). The *Spodoptera frugiperda* (Sf) 9 cells were cultured in TC100 (JRH Biosciences) supplemented with 10% (v/v) FBS and 100 μg/ml kanamycin at 26°C in an incubator. The *Trichoplusia ni* (Tn) 5 cells were cultured in Ex-Cell 405 (JRH Biosciences) at 26°C in an incubator.

PLASMIDS AND RECOMBINANT BACULOVIRUSES

To express annexin A1 as a FLAG-tagged fusion protein in mammalian cells, annexin A1 fragment was amplified from pKK-trc-lipo-155 (a kind gift from Dr. Browning, Biogen) by polymerase chain reaction (PCR) using two oligonucleotides, 5′-TATCCCGG-GAACCACCATGGCAATGGTATCAGAATTCC-3′ and 5′-TATGCGG-CCGCTTACTTATCGTCGTCATCCTTGTAATCGTTTCCTCCACAAAG-AGCC-3′. The FLAG-tag sequence was fused to the C-terminus of the annexin A1 gene in frame. The amplified PCR fragment was digested with *Sma*I and *Not*I, purified, and subcloned into pCAGGS [Niwa et al., 1991], resulting in pCAG-annexin A1-FLAG. To express E6AP and the active-site cysteine-to-alanine mutant of E6AP in mammalian cells, pCAG-HA-E6AP isoform II and pCAG-HA-E6AP C-A were used [Shirakura et al., 2007]. The C-A mutation was introduced at the site of E6AP C843 [Kao et al., 2000]. To express Nedd4, pCAG-HA-Nedd4 was constructed. To make a fusion protein consisting of glutathione S-transferase (GST) fused to the N-terminus of E6AP in *Escherichia coli* (*E. coli*), pGEX-E6AP was used [Shirakura et al., 2007]. Recombinant baculoviruses expressing GST-E6AP were described previously [Shirakura et al., 2007]. To express hexahistidine (His)-tagged annexin A1 in *E. coli*, annexin A1 fragment was amplified from pKK-trc-lipo-155 by PCR using two oligonucleotides, 5′-TATCCCGGGAACCACCATGGCAATGG-TATCAGAATTCC-3′ and 5′-ATAGCGGCCGCGTTTCCTCCACAAA-GAGCC-3′. The PCR fragment was purified and digested with *Sma*I and *Not*I. pET21b was digested with *Nde*I, blunt ended with a DNA blunting kit (Takara, Japan), and digested with *Not*I. Then, the PCR fragment of annexin A1 was ligated into the pET21b fragment, resulting in pET21b-annexin A1. To map the E6AP-binding site on annexin A1 protein, a series of expression plasmids for GST-annexin A1 fusion proteins were constructed by amplifying annexin A1 gene fragments with PCR using sense primers containing *Sma*I site and antisense primers containing a *Not*I site. The amplified PCR fragments were subcloned into pGEM T-Easy (Promega, Madison, WI) and verified by sequencing. Then, the annexin A1 gene fragments were digested with *Sma*I and *Not*I and ligated into the *Sma*I–*Not*I site of pGEX 4T-1 (GE Healthcare, Uppsala, Sweden). The annexin A1 (1-41) gene fragment was amplified from pET21b-annexin A1 by PCR using two oligonucleotides, 5′-TATCCCGG-GAACCACCATGGCAATGGTATCAGAATTCC-3′ and 5′-ATATAGC-GGCCGCTTAGGTAGGATAGGGGCTCACCGCT-3′. The PCR primers used to amplify the annexin A1 fragments were as follows:

Annexin A1 (42–346): 5′-TATCCCGGGAACCACCATGTTCAAT-CCATCCTCGGATGTCG-3′ and 5′-ATATAGCGGCCGCTTAGTTT-CCTCCACAAAGAGCC-3′.

Annexin A1 (42–113): 5′-AAACCCGGGTATGTTCAATCCATCCT-CGGATGTCG-3′ and 5′-TTTGCGGCCGCTTATTTTAGCAGAGC-TAAAACAAC-3′.

Annexin A1 (114–195): 5′-AAACCCGGGTATGACTCCAGCG-CAATTTGATGC-3′ and 5′-TTTGCGGCCGCTTAATTCACACCAA-AGTCCTCAG-3′.

Annexin A1 (196–274): 5′-AAACCCGGGTATGGAAGACTTGG-CTGATTCAG-3′ and 5′-TTTGCGGCCGCTTAGCTTGTGGCGCAC-TTCACG-3′.
Annexin A1 (275–346): 5′-AAACCCGGGTATGAAACCAGCTTT-CTTTGCAGAG-3′ and 5′-ATATAGCGGCCGCTTAGTTTCCTCCA-CAAAGAGCC-3′.
Annexin A1 (42–195): 5′-AAACCCGGGTATGTTCAATCCATCC-TCGGATGTCG-3′ and 5′-TTTGCGGCCGCTTAATTCACACCAAA-GTCCTCAG-3′.
Annexin A1 (114–274): 5′-AAACCCGGGTATGACTCCAGCGCA-ATTTGATGC-3′ and 5′-TTTGCGGCCGCTTAGCTTGTGGCGCAC-TTCACG-3′.
Annexin A1 (196–346): 5′-AAACCCGGGTATGGAAGACTTGG-CTGATTCAG-3′ and 5′-ATATAGCGGCCGCTTAGTTTCCTCCAC-AAAGAGCC-3′.

The sequences of the inserts were extensively verified using an ABI PRISM 3100-Avant Genetic Analyzer (Applied Biosystems, Foster City, CA). To express GST, GST-E6AP, and MEF-E6AP in the baculovirus expression system, recombinant baculoviruses were recovered using a BaculoGold transfection kit (Pharmingen, San Diego, CA) as described previously [Shirakura et al., 2007].

ANTIBODIES

The mouse monoclonal antibodies (MAbs) used in this study were anti-HA MAb (12CA5) (Roche), anti-HA 16B12 MAb (HA.11; BabCO), anti-Annexin I MAb (BD Biosciences, San Jose, CA), anti-glyceraldehyde-3-phosphate dehydrogenase (GAPDH) MAb (Chemicon, Temecula, CA), anti-GST MAb (Santa Cruz Biotechnology, Santa Cruz, CA), anti-ubiquitin MAb (Chemicon), anti-E6AP MAb (E6AP-330) (Sigma), and anti-β-actin MAb (Ab-1) (Calbiochem, San Diego, CA). The polyclonal antibodies (PAbs) used in this study were anti-HA rabbit PAb (Y-11; Santa Cruz Biotechnology), anti-FLAG rabbit PAb (F7425; Sigma), anti-E6AP rabbit PAb (H-182; Santa Cruz Biotechnology), and anti-GST goat PAb (Amersham Bioscience, Buckinghamshire, UK).

IDENTIFICATION OF E6AP-BINDING PROTEINS WITH MALDI-TOF MASS SPECTROMETRY

To screen for potential E6AP-binding proteins, GST pull-down assays were performed using GST-E6AP and ten 225 cm^2-flasks (Corning, New York, NY) of confluent C-33A cells as the source of protein. The cells were lysed in 15 ml of the cell lysis buffer (100 mM Tris-HCl, pH 7.4, 100 mM NaCl, 0.5% Triton X-100 [ICE Biomedicals, Aurora, OH], Complete protease inhibitor cocktail [Roche]). The samples were incubated at 4°C for 1 h, and centrifuged at 13,000*g* for 30 min. The supernatants were collected and pre-cleared with 250 μl of 50% slurry glutathione-Sepharose 4B beads (Amersham Bioscience) to remove proteins that can nonspecifically bind to glutathione-Sepharose 4B beads. The supernatants were then pre-cleared with 250 μg of GST immobilized on glutathione-Sepharose 4B beads to remove proteins which can bind to GST. Then, the supernatant was collected, mixed with 250 μg of GST-E6AP or GST immobilized on glutathione-Sepharose 4B beads, and incubated for 1 h at 4°C. The beads were collected and washed with the cell lysis buffer three times. To remove the bound proteins from GST-E6AP, the bound proteins were released with the releasing buffer (10 mM Tris-HCl, pH 7.4, 150 mM NaCl, 1% sodium deoxycholate, 0.1% sodium dodecyl sulfate [SDS], 1% Triton X-100) five times. The released proteins were mixed with 20% (w/v) trichloroacetic acid (TCA) and incubated at 4°C for 30 min. After centrifugation, the TCA-precipitated samples were washed with ice-cold acetone four times, dried, and lysed in SDS-polyacrylamide gel electrophoresis (SDS-PAGE) loading buffer. The samples were separated by 7.5% SDS-PAGE and stained with Coomassie brilliant blue (CBB). The specific protein bands were excised from the gel and subjected to in-gel trypsin digestion. The tryptic peptide mixtures were analyzed by MALDI-TOF/MS analysis [Kaji et al., 2000]. Prior to MALDI-TOF/MS analysis, the peptide mixtures were desalted using C18 Zip Tips (Millipore, Bedford, MA) according to the manufacturer's instructions. The peptide data were collected in the reflection mode and with positive polarity, using a saturated solution of α-cyano-4-hydroxycinnamic acid (Sigma) in 50% acetonitrile (PE Biosystems, Foster City, CA) and 0.1% trifluoroacetic acid as the matrix. Spectra were obtained using a Voyger DE-STR MALDI-TOF mass spectrometer (PE Biosystems). The database-fitting program MS-Fit at the website (http://jpsl.ludwig.edu.au/ucsfhtml3.4/msfit.htm) of the University of California, San Francisco was used to interpret the MS spectra of the protein digests.

EXPRESSION AND PURIFICATION OF RECOMBINANT PROTEINS

E. coli BL21 (DE3) cells were transformed with plasmids expressing GST fusion protein or His-tagged protein and grown at 37°C. Expression of the fusion protein was induced by 1 mM isopropyl-β-D-thiogalactopyranoside at 25°C for 4 h. Bacteria were harvested, suspended in lysis buffer (phosphate-buffered saline [PBS] containing 1% Triton X-100, Complete protease inhibitor cocktail, EDTA free [Roche]), and sonicated on ice.

Hi5 cells were infected with the recombinant baculoviruses to produce GST-E6AP or GST. GST-E6AP and GST-fusion proteins were purified on glutathione-Sepharose beads (Amersham Bioscience) according to the manufacturer's protocols. His-tagged proteins were purified on Ni-NTA beads (Qiagen, Hilden, Germany) according to the manufacturer's protocols. MEF-E6AP and MEF-E6AP C-A [Shirakura et al., 2007] were purified on anti-FLAG M2 agarose beads (Sigma) according to the manufacturer's protocols.

IMMUNOPRECIPITATION AND IMMUNOBLOT ANALYSIS

Cells were lysed in IP buffer (100 mM Tris-HCl, 100 mM NaCl, pH 7.4, 0.5% Triton X-100, 0.5 mM $CaCl_2$, plus Complete protease inhibitor cocktail, EDTA free) at 4°C for 15 min. Extracts were clarified by centrifugation at 13,000*g* for 20 min, and soluble lysates were pre-cleared with protein G Sepharose (GE Healthcare). The samples were incubated with anti-FLAG M2 agarose (Sigma) and rotated at 4°C for 5 h. The beads were washed five times with IP buffer, and bound proteins were eluted with Laemmli sample buffer. Samples were separated by 10% SDS-PAGE. Immunoblot analysis was performed essentially as described previously [Harris et al., 1999]. The membrane was visualized with SuperSignal West Pico Chemiluminescent Substrate (Pierce, Rockford, IL).

IN VIVO UBIQUITYLATION ASSAY

In vivo ubiquitylation assays were performed essentially as described previously [Shirakura et al., 2007]. Where indicated, cells were treated with 25 μM MG132 (Calbiochem) or with dimethylsulfoxide (DMSO; control) for 30 min prior to collection. FLAG-annexin A1 was immunoprecipitated with anti-FLAG MAb. Immunoprecipitates were analyzed by immunoblotting, using either anti-HA PAb or anti-annexin A1 MAb to detect ubiquitylated annexin A1.

IN VITRO UBIQUITYLATION ASSAY

In vitro ubiquitylation assays were performed essentially as described previously [Shirakura et al., 2007]. For in vitro ubiquitylation of annexin A1, purified GST-annexin A1 was used as a substrate. Purified GST was used as a negative control. Assays were done in 40-μl volumes containing 20 mM Tris–HCl, pH 7.6, 50 mM NaCl, 5 mM ATP, 8 μg of bovine ubiquitin (Sigma), 0.1 mM DTT, 200 ng of mouse E1, 200 ng of E2 (UbcH7), and 0.5 μg of MEF-E6AP, in the presence or absence of $CaCl_2$ as indicated. The reaction mixtures were incubated at 37°C for 120 min followed by immunoblotting.

SIRNA TRANSFECTION

HEK 293T cells (3×10^5 cells in a 6-well plate) were transfected with 40 pmol of either E6AP-specific small interfering RNA (siRNA; Sigma), or scramble negative-control siRNA duplexes (Sigma) using HiPerFect transfection reagent (Qiagen) following the manufacturer's instructions. The E6AP-siRNA target sequences were as follows:

siE6AP-1 (sense) 5′-GGGUCUACACCAGAUUGCUTT-3′; scramble negative control (siCont-1) (sense) 5′-UUGCGGGUCUAAUCACCGATT-3′ [Shirakura et al., 2007]; E6AP-2 (sense), 5′-CAACUCCUGCUCUGAGAUATT-3′; and scramble negative control (siCont-2), 5′-AGACCUACCCGAUUACUGUTT-3′ [Kelley et al., 2005].

ANNEXIN A1 PROTEIN AND E6AP-BINDING ASSAYS

To map the E6AP binding site on annexin A1 protein, GST pull-down assays were performed. A series of recombinant GST-annexin A1 proteins were expressed in *E. coli* and purified using glutathione-Sepharose 4B beads. Equivalent amounts of purified proteins, as estimated by CBB staining, were used for the binding assays. For pull-down assays, purified MEF-E6AP was incubated with GST-annexin A1 proteins immobilized on glutathione-Sepharose 4B beads in 1 ml of the binding buffer (50 mM Tris–HCl [pH 7.4], 150 mM NaCl, 1% Triton X-100, and 5 mM $CaCl_2$) at 4°C for 4 h. The beads were washed four times with binding buffer, and the pull-down complexes were separated by SDS–PAGE on 10% polyacrylamide gels and analyzed by immunoblotting with anti-FLAG MAb.

CYCLOHEXIMIDE (CHX) HALF-LIFE EXPERIMENTS

To examine the half-life of annexin A1 protein, transfected HEK 293T cells were treated with 50 μg/ml CHX at 44 h post-transfection. The cells at time-point zero were harvested immediately after treatment with CHX. Subsequent time points were incubated in medium containing CHX at 37°C for 3, 6, and 9 h as indicated.

CONFOCAL IMMUNOFLUORESCENCE MICROSCOPY

Cells were transfected with pCAG-HA-E6AP C-A and pCAG annexin A1-FLAG using TransIT-LT1 (Takara) according to the manufacturer's instructions. Transfected cells grown on collagen-coated coverslips were washed with PBS, fixed with 4% paraformaldehyde for 30 min at 4°C, and permeabilized with PBS containing 2% FCS and 0.3% Triton X-100. Cells were incubated with anti-HA mouse MAb and anti-FLAG rabbit PAb as primary antibodies, washed, and incubated with Alexa Fluor 488 goat anti-mouse IgG (Molecular Probes, Eugene, OR) and Alexa 555 Fluor goat anti-rabbit IgG (Molecular Probes) as secondary antibodies. Then the cells were washed with PBS, mounted on glass slides, and examined with an LSM510 laser scanning confocal microscope (Carl Zeiss, Oberkochen, Germany).

RESULTS

IDENTIFICATION OF ANNEXIN A1 AS A BINDING PARTNER FOR E6AP

To identify novel substrates for E6AP, we screened for E6AP-binding proteins using pull-down experiments with GST-E6AP. Whole cell lysates from C33-A cells were prepared as described above and incubated with immobilized GST-E6AP or GST alone. After the separation of bound proteins by SDS–PAGE, CBB staining of the gels revealed at least 15 specific bands precipitating with the GST-E6AP. The protein bands were excised from the gel and subjected to in-gel trypsin digestion. The tryptic peptide mixtures were analyzed by MALDI-TOF/MS as described above. Masses obtained using MALDI-TOF were analyzed using the MS-Fit program. This procedure identified seven individual proteins (Fig. 1A,a–g), such as a heat shock protein and a translation elongation factor. One of these bands, migrating at 37 kDa (Fig. 1A,e), was identified as annexin A1 based on six independent MS spectra (Fig. 1B). To verify the interaction of annexin A1 with E6AP, we repeated the pull-down experiments by incubating immobilized GST-E6AP with lysate from C-33A cells. Immunoblot analysis confirmed the proteomic identification of annexin A1 (Fig. 1C).

IN VIVO INTERACTION BETWEEN ANNEXIN A1 AND E6AP

To determine whether the interaction between annexin A1 and E6AP could take place in vivo, annexin A1-FLAG expression plasmid was introduced into HEK 293T cells together with either HA-E6AP expression plasmid or HA-Nedd4 (another HECT domain ubiquitin ligase) [Staub et al., 1996] expression plasmid. A catalytically inactive form of E6AP in which the active site cysteine residue has been substituted with alanine (C843A) was used to avoid potential degradation of interacting proteins. Cells were lysed and annexin A1-FLAG was immunoprecipitated with FLAG-beads. As shown in Figure 2A, HA-E6AP but not HA-Nedd4 was co-immunoprecipitated with annexin A1-FLAG, indicating that E6AP actually interacts with annexin A1 in the cells. We confirmed that the active form of HA-E6AP was also coimmunoprecipitated with annexin A1-FLAG (data not shown).

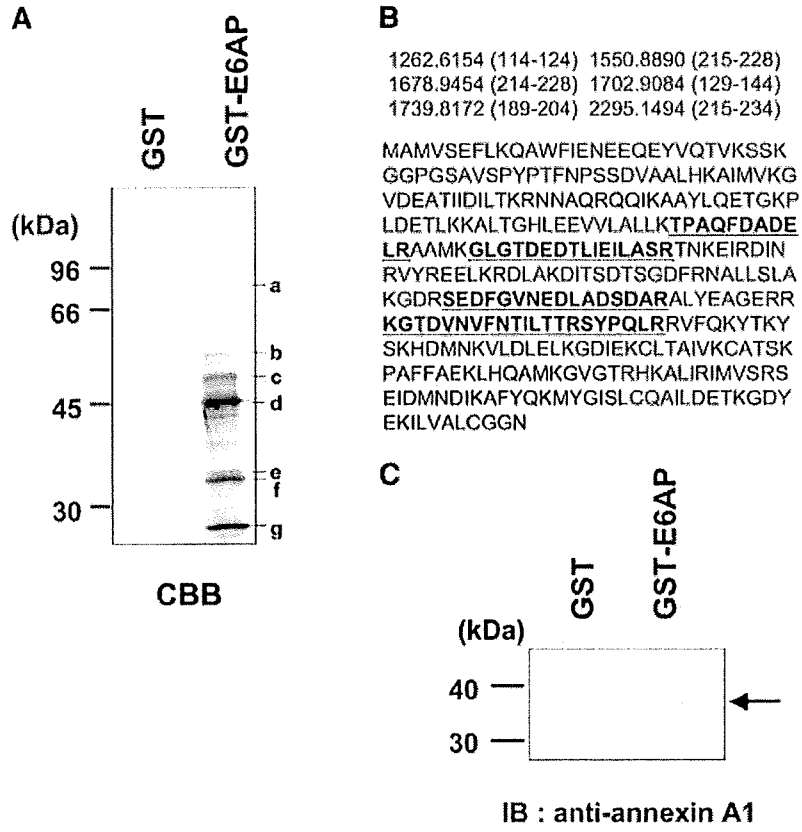

Fig. 1. Identification of annexin A1 as a binding partner for the E6AP. A: GST-E6AP on glutathione-Sepharose beads was incubated with whole-cell extract from C-33A cells. Bound proteins were detected by SDS-PAGE and CBB staining. Molecular weight markers are indicated, as well as the position of p37 (e), which likely corresponds to annexin A1. B: Peptide masses were identified by MALDI-TOF/MS and corresponding amino acids of annexin A1 (trypsin cleavage). Annexin A1 (accession no. 12654863) was identified through MALDI-TOF/MS as a candidate protein interacting with GST-E6AP. The database-fitting program MS-Fit was used to interpret the MS spectra of the protein digests. Six out of 22 masses obtained through the MALDI-TOF analysis corresponded to the theoretical values for annexin A1 cleavage (upper panel, amino acids corresponding to tryptic fragments in brackets) and represented 18% of the proteins' fragments (lower panel, peptides in bold print). The molecular weight search score, MOWSE, was 3.94E + 03. C: The identity of the band shown in panel A as annexin A1 was confirmed by Western blotting with anti-annexin A1 mouse MAb.

To determine whether annexin A1 and E6AP co-localize in the cells, immunofluorescence microscopy analysis was performed in two different cell lines, HEK 293T cells and C-33A cells. The immunofluorescence study showed that E6AP partially co-localized with annexin A1 in the cytoplasm of both types of cells (Fig. 2B).

To determine whether endogenous E6AP interacts with endogenous annexin A1 in vivo, C-33A cells were lysed and subjected to immunoprecipitation with anti-annexin A1 antibody or anti-E6AP antibody. Endogenous E6AP was co-immunoprecipitated with anti-annexin A1 antibody, but not with control antibody (Fig. 2C, left panel, upper lane). Moreover, endogenous annexin A1 was co-immunoprecipitated with anti-E6AP antibody, but not with control antibody (Fig. 2C, right panel, lower lane). These results suggest that endogenous E6AP can interact with endogenous annexin A1 in C-33A cells.

E6AP DECREASES STEADY-STATE LEVELS OF ANNEXIN A1 PROTEIN

To determine whether E6AP functions as an E3 ubiquitin ligase for the ubiquitylation of annexin A1, we assessed the effects of E6AP on annexin A1 protein in HEK 293T cells. The annexin A1-FLAG expression plasmid together with the plasmid for HA-tagged wild-type E6AP, catalytically inactive mutant E6AP, E6AP C-A, or Nedd4, was introduced into HEK 293T cells, and the levels of annexin A1 proteins were examined by immunoblotting. The steady-state levels of annexin A1 protein decreased with an increase of the E6AP plasmids (Fig. 3A,B). However, neither E6AP C-A nor Nedd4 decreased the steady-state levels of the annexin A1 protein, suggesting that E6AP enhances the degradation of annexin A1 protein.

E6AP ENHANCES THE DEGRADATION OF ANNEXIN A1 PROTEIN

To determine whether the E6AP-induced reduction of the annexin A1 protein is due to an increase in the rate of degradation of annexin A1 protein, we examined the degradation of annexin A1 using the protein synthesis inhibitor CHX. Annexin A1 together with wild-type E6AP or inactive mutant E6AP C-A was expressed in HEK 293T cells. At 44 h after transfection, the cells were treated with either 50 μg/ml CHX alone or 50 μg/ml CHX plus 25μM MG132 to inhibit

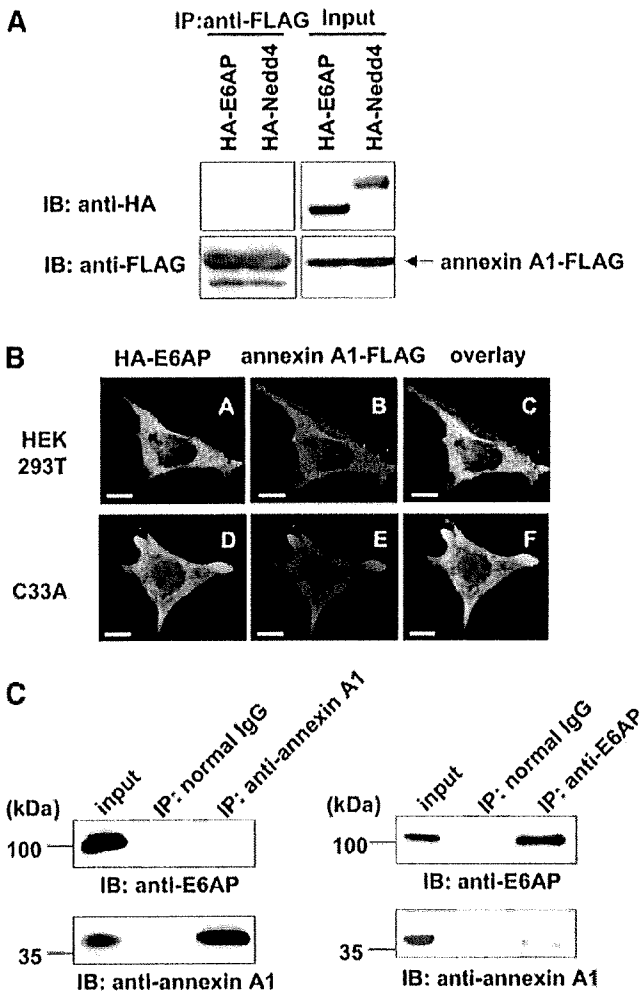

Fig. 2. In vivo interaction between annexin A1 and E6AP. A: HEK 293T cells were co-transfected with pCAG-annexin A1-FLAG together with pCAG-HA-E6AP C-A or pCAG-HA-Nedd4. The cell lysates were immunoprecipitated with FLAG beads and analyzed by immunoblotting with anti-HA PAb or anti-FLAG PAb. B: HEK 293T cells and C-33A cells were transfected with either HA-E6AP plasmid or annexin A1-FLAG plasmid, grown on coverslips, fixed, and processed for double-label immunofluorescence for HA-E6AP or annexin A1-FLAG. All the samples were examined with an LSM510 laser scanning confocal microscope (bar, 10 μm). C: C33A cells were lysed in the cell lysis buffer. The cell lysates were immunoprecipitated with anti-annexin A1 mouse MAb or control normal mouse IgG and analyzed with anti-E6AP mouse mAb or anti-annexin A1 mouse MAb as indicated (left panel). The cell lysates were immunoprecipitated with anti-E6AP mouse mAb or control normal mouse IgG and analyzed with anti-E6AP mouse mAb or anti-annexin A1 mouse mAb as indicated (right panel).

proteasome function. Cells were collected at 0, 3, 6, and 9 h following the treatment and analyzed by immunoblotting (Fig. 4A). Overexpression of E6AP resulted in rapid degradation of the annexin A1 protein, whereas the annexin A1 protein was stable in the cells transfected with inactive mutant E6AP C-A. Treatment of the cells with MG132 inhibited the degradation of annexin A1 (Fig. 4A). These results suggest that E6AP enhances proteasomal degradation of annexin A1.

KNOCKDOWN OF ENDOGENOUS E6AP BY SIRNA RESULTS IN ACCUMULATION OF ENDOGENOUS ANNEXIN A1 PROTEIN

To determine whether or not E6AP is critical for the degradation of endogenous annexin A1 protein, the expression of E6AP was knocked down by siRNA and the expression of annexin A1 and E6AP was analyzed by immunoblotting. We used two different siE6AP duplexes, siE6AP-1 and siE6AP-2, to knockdown the endogenous E6AP. Transfection of either siE6AP-1 or siE6AP-2 into HEK 293T cells resulted in a decrease in E6AP levels by 70–95% (Fig. 4B, the first panel), indicating that both siRNAs against E6AP resulted in a remarkable decrease in the protein level of E6AP. Knockdown of endogenous E6AP resulted in an accumulation of the endogenous annexin A1 protein, but no accumulation of the endogenous annexin A2 protein (Fig. 4B, the second and third panels), suggesting that the ubiquitylation and degradation of endogenous annexin A1 is specifically inhibited by knockdown of endogenous E6AP in vivo. These results suggest that endogenous E6AP plays a role in the proteolysis of endogenous annexin A1.

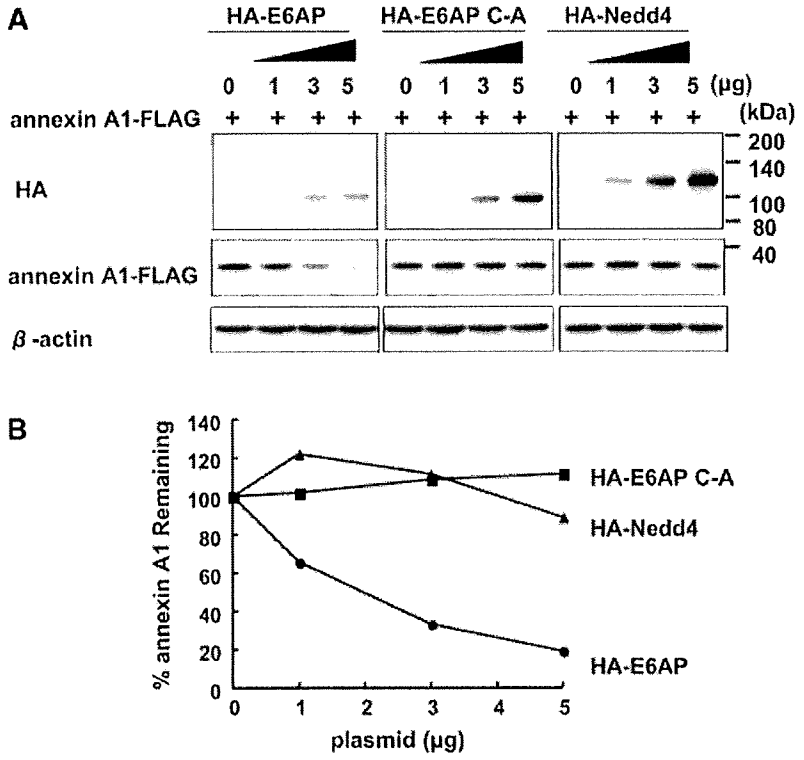

Fig. 3. E6AP decreases steady-state levels of annexin A1 protein in HEK 293T cells. HEK 293T cells (1×10^6 cells/10-cm dish) were transfected with 1 μg of pCAG annexin A1-FLAG along with either pCAG-HA-E6AP, pCAG-HA-E6AP C-A, or pCAG-HA-Nedd4 as indicated. At 48 h post-transfection, protein extracts were separated by SDS-PAGE and analyzed by immunoblotting with anti-HA PAb (top panel), anti-FLAG MAb (middle panel), and anti-β-actin MAb (bottom panel). B: Quantitation of data shown in panel A. Intensities of the gel bands were quantitated using the NIH Image 1.62 program. The level of β-actin served as a loading control. Circles, E6AP; squares, E6AP C-A; triangles, Nedd4.

E6AP MEDIATES UBIQUITYLATION OF ANNEXIN A1 IN VIVO

To determine whether E6AP can induce ubiquitylation of annexin A1 in cells, we performed in vivo ubiquitylation assays. HEK 293T cells were transfected with annexin A1-FLAG plasmid and either E6AP or Nedd4 plasmid, together with a plasmid encoding HA-tagged ubiquitin to facilitate the detection of ubiquitylated annexin A1 protein. Cell lysates were immunoprecipitated with anti-FLAG MAb and immunoblotted with anti-HA PAb to detect ubiquitylated annexin A1 protein. Only a faint ubiquitin signal was detected in the cells co-transfected with empty plasmid or Nedd4 plasmid (Fig. 5A, lanes 4 and 6). In contrast, co-expression of E6AP led to readily detectable ubiquitylated forms of the annexin A1 as a smear of higher-molecular-weight bands (Fig. 5A, lane 5). Immunoblot analysis with anti-FLAG PAb confirmed that annexin A1-FLAG proteins were immunoprecipitated and that higher-molecular-weight bands conjugated with HA-ubiquitin were indeed ubiquitylated forms of the annexin A1 proteins (Fig. 5B, lane 5). These results suggest that E6AP enhances ubiquitylation of annexin A1 in the cells.

E6AP MEDIATES UBIQUITYLATION OF ANNEXIN A1 IN VITRO

To reconstitute the E6AP-mediated ubiquitylation of annexin A1 in vitro, we performed an in vitro ubiquitylation assay of the annexin A1 using purified MEF-E6AP and GST-annexin A1 as described above. When the in vitro ubiquitylation reaction was carried out either in the absence of MEF-E6AP or in the presence of MEF-E6AP C-A, no ubiquitylation signal was detected (Fig. 5C, lanes 4 and 5). However, inclusion of purified MEF-E6AP in the reaction mixture resulted in ubiquitylation of GST-annexin A1 (Fig. 5C, lane 6), while no ubiquitylation was observed in the absence of ATP (Fig. 5C, lane 7). No signal was detected when GST was used as a substrate (data not shown). These results indicate that E6AP directly mediates ubiquitylation of annexin A1 protein in an ATP-dependent manner.

Ca^{2+}-DEPENDENT INTERACTION BETWEEN ANNEXIN A1 AND E6AP

We next assessed the effects of Ca^{2+} on the interaction between annexin A1 and E6AP. We performed the pull-down experiments by incubating immobilized GST-E6AP or GST alone with purified His-tagged annexin A1 in the presence or absence of 1 mM $CaCl_2$. After precipitation and SDS-PAGE, the bound annexin A1 was detected by immunoblotting with anti-annexin A1 antibody. GST-E6AP, but not GST, was able to precipitate annexin A1 only in the presence of Ca^{2+} (Fig. 6A, lane 4). These interactions were dependent on the concentration of Ca^{2+}, as increasing concentrations of Ca^{2+} resulted in an increase of binding of annexin A1 to E6AP (Fig. 6B). These